

This is to certify that the thesis entitled

Microbial Ecology of the Mammalian Gastrointestinal Tract: The Effects of Pathogen Colonization, Genotype, and Antibiotics on the Mucosa-associated Microbiota of Mice

presented by

Heather D. Wood

has been accepted towards fulfillment of the requirements for the

M.S. degree in Cell and Molecular Biology

Major Professor's Signature

22 AUG 2006

Date

MSU is an Affirmative Action/Equal Opportunity Institution

PLACE IN RETURN BOX to remove this checkout from your record. **TO AVOID FINES** return on or before date due. **MAY BE RECALLED** with earlier due date if requested.

DATE DUE	DATE DUE	DATE DUE	

5/08 K:/Proj/Acc&Pres/CIRC/DateDue.indd

MICROBIAL ECOLOGY OF THE MAMMALIAN GASTROINTESTINAL TRACT: THE EFFECTS OF PATHOGEN COLONIZATION, GENOTYPE, AND ANTIBIOTICS ON THE MUCOSA-ASSOCIATED MICROBIOTA OF MICE

Ву

Heather D. Wood

A THESIS

Submitted to
Michigan State University
in partial fulfillment of the requirements
for the degree of

MASTER OF SCIENCE

Cell and Molecular Biology

2006

ABSTRACT

MICROBIAL ECOLOGY OF THE MAMMALIAN GASTROINTESTINAL TRACT: THE EFFECTS OF PATHOGEN COLONIZATION, GENOTYPE, AND ANTIBIOTICS ON THE MUCOSA-ASSOCIATED MICROBIOTA OF MICE

By

Heather D. Wood

The microbiota is a vastly understudied complex community of microbes. It has been implicated in inflammatory diseases such as arthritis and inflammatory bowel disease. The effects of various ecological stressors on the microbial community of the gastrointestinal tract were determined by utilizing non-culture based techniques and ecological diversity measures. Together our results indicate that the community structure of the indigenous mucosal microbiota can be determined and followed by the use of non culture-based techniques. More importantly, comparison between multiple animals suggests that ecologic stressors (e.g. alterations in host genotype, antibiotic administration and invasion by a pathogen) can result in drastic and reproducible alteration in the community structure. If we were to develop a greater understanding of the factors that shape and maintain the structure of the indigenous microbiota of the gut, this should result in novel treatment modalities for inflammatory diseases based on rationale manipulation of the intestinal microbiota.

ACKNOWLEDGEMENTS

I would like to express very sincere gratitude for the guidance and support of my research mentor Dr. Vincent Young. I would also like to acknowledge the other members of my laboratory (Alicia Cotey, Jason Pratt, Jennifer Ellis-Cortez, Ju Young Chang, Nabeetha Nagalingam, Dion Antonopoulos, John Wertz and Shelby Newman) for their friendship and assistance with my experiments. I am grateful for the insight of my committee members (Dr. Tom Whittam, Dr. Tom Schmidt, and Dr. Linda Mansfield). Of course I would like to acknowledge all of my friends and my very supportive family, especially my husband Randy Wood.

TABLE OF CONTENTS

LIST OF TABLES	V
LIST OF FIGURES	vi
CHAPTER 1- Introduction	
Intestinal microbiota	2
Crohn's disease	
Microbiota and IBD	
Host immune system and IBD	
Animal models of IBD	
Conclusion	8
CHAPTER 2- Colonization of the Cecal Mucosa by Wild-type and Mutant H. hepaticus	
Summary	11
Introduction	
Materials and methods	
Results	_
Discussion.	
CHAPTER 3- The Effect of Host Genotype on the Composition of the Cecal- mucosa associated microbiota of Sibling C57BL/6 IL-10+/+ and IL-10-/- Mice Summary	55 56 57
CHAPTER 4- The Effect of Antibiotic Treatment on the Composition of th	
Summary	77
Introduction	
Materials and methods	
Results	
Discussion	99
CHAPTER 5- Summary and Synthesis	107
REFERENCES	112

LIST OF TABLES

Table 1. A description of the number of animals used for the 6-week time course and 2 week infection studies
Table 2. Primer sequences24
Table 3. Diversity statistics for each of the clone libraries from IL-10-/-, IL-10+/-, and IL-10+/+ at 4, 11, and 19 weeks of
age69
Table 4. The percent proportion of the sequences that were classified into phyla by the Ribosomal Database Project Libcompare for each of the IL-10-/-, IL-10+/-, and IL-10+/+ samples at 4, 11, and 19 weeks of age
Table 5. ∫ -LIBSHUFF was used to make all pair-wise comparison between the 13 clone libraries from the IL-10-/-, IL-10+/+, and IL-10-/+ littermates at 4, 11 and 19 weeks of age
Table 6. \(\) -LIBSHUFF was used to make all pair-wise comparison between the 15 clone libraries from the untreated (U), streptomycin treated (S), and the triple antibiotic treated (TA) animals
Table 7. The percent proportion of the sequences classified into phyla by the Ribosomal Database Project Libcompare for each of the 15 clone libraries.
iiDraries98

LIST OF FIGURES

Figure 1. Representative T-RFLP traces comparing the mucosa-associated microbiota in the cecae of an uninfected C57BL/6 mouse and two mice infected with <i>H. hepaticus</i> 30 days previously
Figure 2. Changes in diversity measures of the mucosal-associated microbiota of the murine cecum 30 days after experimental infection with <i>H. hepaticus</i>
Figure 3. Phylogenetic tree showing the distribution of 16S rDNA sequences from clone libraries constructed from cecal DNA samples obtained from an uninfected mouse (green circles) or a mouse 30 days after infection with <i>H. hepaticus</i> (red squares)
Figure 4. Comparison between T-RFLP analysis and in silico terminal restriction fragment length polymorphism analysis
Figure 5. Representative T-RFLP traces temporally monitoring the establishment of colonization in the murine cecum by <i>H. hepaticus</i>
Figure 6. Summary of the temporal monitoring of the colonization of the cecae of mice by <i>H. hepaticus</i>
Figure 7. Temporal development of typhlocolitis in IL-10-/- mice infected with wild-type <i>H. hepaticus</i> or a CDT-deficient isogenic mutant
Figure 8. Monitoring the colonization of IL-10-/- mice with <i>H. hepaticus</i> 41
Figure 9. UPGMA dendrogram created using Bray-Curtis distances (1-Bray-Curtis) calculated from T-RFLP analysis of <i>H. hepaticus</i> infected versus uninfected KO (IL-10-/-) and WT (IL-10+/+)
mice

Figure 10. UPGMA dendrogram created using Bray-Curtis distances (1-Bray-Curtis) calculated from T-RFLP analysis of <i>H. hepaticus</i> infected versus uninfected KO (IL-10-/-) and WT (IL-10+/+) mice with the <i>H. hepaticus</i> TRF removed
Figure 11. UPGMA dendrogram created using Bray-Curtis distances (1-Bray-Curtis) calculated from T-RFLP analysis of (KO) IL-10-/-, (WT) IL-10+/+, and (HET) IL-10-/+ littermates and their mothers
Figure 12. UPGMA dendrogram created using Bray-Curtis distances (1-Bray-Curtis) calculated from clone library analysis of IL-10-/-, IL-10+/+, and IL-10-/+ littermates
Figure 13. Representative T-RFLP traces for untreated, streptomycin treated, and triple antibiotic treated animals
Figure 14. UPGMA dendrogram created using Bray-Curtis distances (1-Bray-Curtis) calculated from T-RFLP analysis of IL-10-/- mice treated with antibiotics compared to untreated controls
Figure 15. UPGMA dendrogram created using Bray-Curtis distances (1-Bray-Curtis) calculated from clone library analysis of IL-10-/- mice treated with antibiotics compared to untreated controls
Figure 16. Rarefaction curves representing the richness of the mucosa- associated microbiota in untreated animals compared to antibiotic treated animals

Chapter 1

Introduction

Intestinal Microbiota

The microbiota of the gastrointestinal tract is a highly complex community (interacting microbial members of different species) of microbes of over 400 different species (25). A large-scale study of human intestinal microbiota of 11,831 bacterial 16S rDNA sequences identified 395 phylotypes divided into 9 phyla (25). Eckberg et al. found that most phylotypes were members of the *Firmicutes* and *Bacteriodetes* phyla (25). A murine microbiota study of 5,088 bacterial 16S rDNA sequences showed that even though 85% of the sequences represented phylotypes not detected in humans there is substantial similarity between human and murine microbiotas at the phylum level (63). As seen in the human gut, a majority of the phylotypes in the murine gut fall within the *Firmicutes* and *Bacteriodetes*.

It is estimated that up to 60% of the organisms in the gut cannot be cultivated (107). Over the past decade, molecular-based approaches have revealed enormous phylogenetic diversity in the microbial world that is not yet represented in culture. This information has come almost entirely by retrieval of small subunit (SSU) rRNA sequence information, which provides phylogenetic context in which to quantify such diversity. Therefore, in order to study the microbiota, non-culture based techniques using the conserved 16S rDNA sequence, such as T-RFLP and clone library analysis are used. These non-culture based techniques have been traditionally used to study environmental microbial ecology. However, it is becoming increasingly common to utilize these

methods to study the microbial communities of humans (e.g. vaginal tract, oral cavity, and intestinal tract (51, 94, 95, 114).

Sequences obtained from 16S rDNA clone library analysis can be used for phylogenetic analysis. The Ribosomal Database Project - II (RDP-II) in the Center of Microbial Ecology at Michigan State University (MSU) contains over 250,000 16S rRNA sequences along with many useful online analysis tools (http://rdp.cme.msu.edu). This enables one to easily analyze 16S rRNA sequences obtained from the community being studied. 16S rDNA sequences can be used to calculate diversity by measuring the richness (total number of species) and evenness (relative abundance of each species) of the microbial community. Standard ecological measures of diversity can be computed with the aid of computer programs such as Distance-Based OTU and Richness (DOTUR) and EstimateS (http://viceroy.eeb.uconn.edu/EstimateS) (99). Programs are also available to compare the evenness and richness of several libraries at once such as (-LIBSHUFF (38). The availability of such tools allows one to use ecological measures to determine the impact on the microbial community when subjected to ecological stresses, to compare communities to one another with presence/absence of shared species and the relative abundances of those species, and to eventually relate structure of the community to function.

The microbiota serves many important functions in the gut, including vitamin synthesis, short chain fatty acid production, and colonization resistance (7, 76, 115). Though beneficial the host must still have barriers against the

microbiota. The gastrointestinal epithelium, mucosal layer, and the innate and acquired immune system serve as such barriers. There is a stable relationship between these host barriers and the microbiota. If there is an alteration or missing component in this relationship pathology could occur such as asthma (54, 81, 82, 110), arthritis (110, 112) and inflammatory bowel disease (IBD) (9, 70).

Crohn's disease

It is estimated over one million Americans suffer from IBD. Crohn's disease and ulcerative colitis are collectively known as IBD. The inflammatory bowel disease, Crohn's disease, is characterized by an exaggerated Th 1 response that can occur anywhere in the digestive tract. Overall symptoms include severe bouts of diarrhea, abdominal pain, and narrowing of the intestinal lumen potentially leading to bowel obstructions. Treatment for Crohn's typically involves anti-inflammatory and immunosuppressant drugs and often times, surgery. Clinical studies of the effectiveness of antibiotics and probiotics have led to varied results demonstrating the complexity of treating this disease (42, 97, 98).

Although the etiology of Crohn's disease is not known, a unifying hypothesis is that it is caused by a dysregulated mucosal immune response to the normal microbiota in genetically predisposed individuals (69, 73). This may reflect a combination of defects in intestinal barrier function leading to overexposure to antigens of the resident microbiota, loss of immune tolerance to

the resident microbiota, loss of immune tolerance to the resident microbiota, or an imbalance between protective versus harmful intestinal bacteria (dysbiosis). Overall, it is clear that IBD involves a complex interaction of environmental and genetic factors between the host and its resident microbiota.

Microbiota and IBD

Crohn's patients have a Th1 exaggerated immune response to their own microbiota and IBD develops in the areas of highest bacterial concentration, thus incriminating the microbiota in the initiation of disease (30). Additionally, diversion of the fecal stream is associated with distal improvements in IBD patients (30). Studies show there are differences in the mucosa-associated bacteria in IBD patients compared to controls. A reduction in diversity with loss of beneficial organisms such as Lactobacillus and Bifidobacterium and an increase in mucosa-associated bacteria and invasion occur in IBD patients (57, 72, 79, 85, 90). If disruption of the microbiota's stability is in fact a contributing factor to the pathogenesis of IBD then a better understanding of this phenomenon will lead to better treatment options. The use of antibiotic and probiotic (live microorganisms that confer benefit to the host when consumed) regimens exert beneficial effects in humans and animal models (42, 67, 74, 88). Additionally, it is not clear whether microbiota instability is a cause or an effect of disease, thus warranting further investigation.

Once established, the microbiota is generally stable throughout a person's life but it is subjected to external insults continuously. These insults include such

things as food borne pathogens and antibiotic treatment. Antibiotic associated diarrhea (AAD) is an example of a situation when the homeostasis of the microbiota is disrupted (123). In a normal healthy individual the community returns back to "normal" after a period of time (123). This may not be the case in an individual that has an immune system abnormality. This individual may be more prone to disruptions in the microbiota. For example, the "hit and run" hypothesis states that the introduction of a pathogen may be enough to trigger IBD in some genetically susceptible people (105). Disease could result from the pathogen causing disturbances in the microbiota. A recent study demonstrated that the introduction of a murine pathogen caused perturbations in the mucosal-associated microbiota of a C57BL/6 wild-type mouse (58).

Host Immune system and IBD

A defect in the acquired or innate immune system may lead to the chronic inflammation seen in IBD (8). Failure of regulatory lymphocytes and associated cytokines (e.g.IL-10 and TGF-ß) or exaggerated activity of effector lymphocytes could lead to the chronic inflammatory response seen in IBD (39, 106). Failure of the innate immune system has been implicated due to studies of mutations affecting the bacterial pattern recognition receptors such as the membrane bound Toll-like receptors (TLRs) 2 and 4 and the cytoplasmic nucleotide-binding oligomerization domain 2 (NOD 2) (2, 3, 14, 17). These receptors recognize common components of bacteria such as lipopolysaccharide and peptidoglycan. At least 7 loci have been identified to confer susceptibility to IBD (73). The most

studied is the NOD2 mutation. It is estimated that 1/3 of individuals with Crohn's disease have a mutation in the NOD2 gene. Interestingly not all individuals with a NOD2 mutation end up with Crohn's disease. Therefore, environmental factors must also be involved such as the microbiota.

Animal models of IBD

There are several mouse models that demonstrate an alteration in the innate immune system, adaptive immune system, or damage to the epithelium, in addition to the presence of the microbiota causes murine IBD (26). This is further supported by the fact that none of these animal models develop disease when maintained in germ-free conditions. One such model is a C57BL/6 IL-10-/- (interleukin-10 knock-out) mouse infected with *H. hepaticus* (an enterhepatic *Helicobacter* species that naturally infects the distal gastrointestinal tract of mice). (59).

IL-10 is an important anti-inflammatory cytokine involved in innate and adaptive immunity. Introducing *H. hepaticus* into the gut microbiota of C57BL/6 IL-10-/- mouse elicits an exaggerated Th1 response leading to severe typhilitis/colitis. Therefore, this mouse model is commonly employed as a model of Crohn's disease. These IL-10-/- mice remain disease free until the introduction of *H. hepaticus*. One study even demonstrated that IL-10-/- mouse monoassociated with *H. hepaticus* did not develop disease (23). When challenged with *H. hepaticus* wild-type C57BL/6 animals from the same colony do not develop

typhilitis/colitis. This demonstrates the relationship between genetic background and an environmental factor (microbiota) in IBD.

Conclusion

The microbiota of the gastrointestinal tract is a vastly understudied microbial community. A greater understanding of the factors that shape and maintain the structure of the intestinal microbiota should lead to novel treatment options for diseases related to a dysbiotic state of the microbiota. This would be based on rational manipulation of the intestinal microbiota.

It is widely accepted that Crohn's disease is a complex disease caused by an abnormal immune response to the members of the intestinal microbial community. Studies have implicated the microbiota in both human and mouse IBD. In our laboratory we are studying the development of IBD in C57BL/6 IL-10-/- mice maintained in our specific pathogen free (SPF) colony at MSU they remain disease free until the introduction of *H. hepaticus*. Wild-type C57BL/6 animals from the same colony do not develop typhilitis/colitis when challenged with *H. hepaticus*. This IBD animal model was utilized to investigate the dynamics of the microbiota. Non-culture based techniques utilizing 16S rDNA, T-RFLP and clone library analysis, along with measures of community diversity, were used in this study to follow the changes in the intestinal microbiota brought on by invasion of a pathogen, changes in host genotype, and antibiotic treatment. This knowledge could be used to design future research involving the manipulation of

the microbiota to alleviate not only IBD but also other inflammatory diseases such as asthma, and arthritis (65, 81, 82, 112).

Chapter 2

Colonization of the Cecal Mucosa By Wild-type and Mutant

Strains of Helicobacter hepaticus

Parts of this chapter were published in: Kuehl, C. J., H.D. Wood, T.L. Marsh, T.M. Schmidt, and V.B. Young. 2005. "Colonization of the Cecal Mucosa by Helicobacter hepaticus Impacts the Diversity of the Indigenous Microbiota."

Infection and Immunity; 73 (10): 6952-6961.

Parts of this chapter were published in: Pratt, J.S., K.L. Sachen, H.D. Wood, K.A. Eaton, and V.B. Young. 2006. "Modulation of Host Immune Responses by the Cytolethal Distending Toxin of *Helicobacter hepaticus*." Infection and Immunity; 74 (8): 4496-4504.

Summary

Establishment of mucosal and/or luminal colonization is the first step in the pathogenesis of many gastrointestinal bacterial pathogens. The pathogen must be able to establish itself in the face of competition from the complex microbial community that is already in place. We used culture-independent methods to monitor the colonization of the cecal mucosa of *Helicobacter*-free mice following experimental infection with the pathogen, Helicobacter hepaticus. Two days after infection, H. hepaticus comprised a minor component of the mucosa-associated microbiota, but within 14 days became the dominant member of the community. Colonization of the mucosa by *H. hepaticus* was associated with a decrease in the overall diversity of the microbial community, in large part due to changes in evenness resulting from the relative dominance of *H. hepaticus* as a member of the community. Our results demonstrate that invasion of the complex gastrointestinal microbial community by a pathogenic microorganism causes reproducible and significant disturbances in the community structure. The use of non culture-based methods to monitor these changes should lead to a greater understanding of the ecological principles that govern pathogen invasion and may lead to novel methods for the prevention and control of gastrointestinal pathogens. Persistent murine infection with Helicobacter hepaticus leads to chronic gastrointestinal inflammation and neoplasia in susceptible strains. To determine the role of the virulence factor cytolethal distending toxin (CDT) in the pathogenesis of this organism, IL-10^{-/-} mice were experimentally infected with

wild-type *H. hepaticus* and a CDT-deficient isogenic mutant. Both wild-type *H. hepaticus* and the CDT-deficient mutant successfully colonized IL-10^{-/-} mice, and reached similar tissue levels by six weeks after infection. Only animals infected with wild-type type *H. hepaticus* developed significant typhlocolitis. Additionally, to determine the effect of inflammation on the mucosa-associated microbiota IL-10-/- and wild-type mice were experimentally infected with both wild-type *H. hepaticus* and a CDT-deficient isogenic mutant. Not only does experimental infection and host genotype have an effect on the microbial community but inflammation also appears to have an effect.

Introduction

The gastrointestinal (GI) tract of mammals is inhabited by a complex microbial community that plays a crucial role in maintaining GI tract homeostasis (7, 76). The GI microbiota can perform a variety of beneficial metabolic functions including the catabolism of complex carbohydrates to yield short chain fatty acids such as butyrate (91). The gut microbiota also directly interacts with the intestinal mucosa, aiding in the development of the mucosal epithelium and maturation of the mucosal immune system (52).

Another beneficial function of the indigenous GI microbiota is to provide resistance to colonization by pathogenic microorganisms, a defense mechanism commonly referred to as "colonization resistance" (12, 36, 115). Although there is wide variation in the specific composition of the climax microbial community of the GI tract between individuals, within an individual the climax community appears to be relatively stable over time (50, 124). This stability is reflected in the development of colonization resistance. In spite of colonization resistance, certain pathogenic bacteria are able to establish residence in the gastrointestinal tract despite the presence of the indigenous microbiota. It is not known if the introduction of an "invasive species" causes detectable changes to the overall ecologic structure of the intestinal microbial community.

Helicobacter species are responsible for chronic human and veterinary infections (104). In humans, *H. pylori* infection can last for decades, associated with a subclinical gastritis. Long-term infection with *H. pylori* can lead to the

development of neoplastic disease including gastric cancer and mucosalassociated lymphoid tissue lymphomas (87).

In addition to *H. pylori* and other gastric *Helicobacter* species, the enterohepatic *Helicobacter* species (EHS) have emerged as veterinary and human pathogens also associated with long-term infection and the development of neoplastic disease (34, 104). The EHS *H. hepaticus* was originally discovered as the causative agent for the development of chronic hepatitis and hepatocellular cancer in A/JCr mice (35, 117). It was subsequently determined that *H. hepaticus* infection in mice with altered immune function was also associated with the development of a condition that mimicked human inflammatory bowel disease (IBD) (16, 19). Long-term infection with *H. hepaticus* in animals that develop IBD can lead to the development of colon cancer (27, 28, 68).

H. hepaticus and a number of other EHS have been shown to produce a cytotoxin that is a member of the cytolethal distending toxin (CDT) family (18, 120, 122). CDT is a tripartite bacterial toxin that is encountered in a number of pathogenic Gram-negative organisms including Campylobacter jejuni and other Campylobacter species, certain Escherichia coli strains, Shigella dysenteriae, Haemophilus ducreyi, and Actinobacillus actinomycetemcomitans (reviewed in (61, 83, 84)).

The examination of complex consortia of bacteria has been transformed by the development of culture-independent methods to determine the

composition and structure of the community (86). In large part, this has been accomplished through the retrieval of small subunit (SSU) rRNA gene sequence, which provides a phylogenetic context in which to describe the diversity of the community. Several methods have been developed to examine the SSU rRNA-encoding gene (i.e. the SSU rDNA) (33). One method is to directly amplify DNA extracted from a community using primers that target the conserved regions of the SSU rDNA. These amplicons are then cloned and the sequence of a number of these clones determined.

While rDNA sequencing provides unambiguous phylogenetic identification, the richness of many microbial communities and the laboriousness of the technique makes this approach unwieldy when applied to a large number of communities. Hence, other approaches, such as terminal restriction fragment length polymorphism (T-RFLP), were developed as rapid methodologies with high throughput that are more suitable for this type of analysis (71). T-RFLP targeting SSU rDNA (5, 6) has been used to profile complex microbial communities (15, 20, 64). Although phylogenetic identification of specific members of a community is difficult, T-RFLP can rapidly provide information regarding the richness and evenness of a complex community.

In this study we followed the community structure of the mucosaassociated microbiota of the murine cecum during the establishment of colonization by a wild-type (CDT+) and mutant (CDT-) of the murine pathogen *Helicobacter hepaticus* (108). We used T-RFLP analysis and 16S rDNA clone library construction to provide the first detailed examination of the microbial ecology of the GI tract during invasion by a bacterial pathogen.

Materials and Methods

Animals and housing.

The initial infection studies were performed with C57BL/6 animals purchased from the Jackson Laboratories (Bar Harbor, ME). For subsequent experiments, a breeding colony of wild type (IL-10+/+) and IL-10-/- C57BL/6 mice was established using breeding stock purchased from the Jackson Laboratories. All animal protocols were reviewed and approved by the Michigan State University All University Committee on Animal Use and Care. Mice were housed with autoclaved food, bedding and water. Cage changes were performed in a laminar flow hood. Animals were housed in groups of up to 4 animals per microisolator cage and animals experienced a cycle of 12 hours of light and 12 hours of darkness. See Table 1 for number of animals used for each experiment.

Helicobacter hepaticus and growth conditions.

The type stain of *H. hepaticus*, strain 3B1 (ATCC 51449) was obtained from the American Type Culture Collection (ATCC), Manassas, VA. The isogenic mutant 3B1::Tn20 was generated by transposon shuttle mutagenesis with allelic exchange into *H. hepaticus* (121). 3B1::Tn20 has a transposon inserted near the start of *cdtA* and no longer produces cytolethal distending toxin (121).

H. hepaticus was cultured on trypticase soy agar plates containing 5% sheep blood A microoxic environment was maintained in vented GasPak jars without catalyst which were evacuated to -20 mm Hg and then equilibrated with a gas mixture consisting of 80% N₂, 10% H₂, and 10% CO₂. An incubation temperature of 37°C was used for growth. *H. hepaticus* suspensions for animal challenge were prepared by harvesting organisms from culture plates into trypticase soy broth (TSB).

Experimental Mouse Infection.

4-6 week old C57BL/6 wild type mice were challenged orally with 1 $O.D._{600nm}$ (approximately 1 x 10^8 cfu) of a suspension of *H. hepaticus* in TSB. Control animals were given 300 μ l of sterile TSB. The *H. hepaticus* suspension and the TSB control were administered directly into the stomach using a 24-gauge ball-tipped gavage needle. Infected and control groups of mice were kept in separate cages.

Monitoring of Colonization.

The colonization status of *H. hepaticus*-infected animals was monitored weekly by culture and PCR analysis of fecal pellets taken from three mice in each experimental group as described previously.

Necropsy and microbiological culture.

Mice were euthanized by CO₂ asphyxiation. The tip of the cecum of each mouse was removed, quartered, and washed in phosphate buffered saline to remove luminal contents. Three sections were snap frozen in dry ice/ethanol and one section was cultured on CVA selective agar plates (20mg/ml cefoperazone, 10mg/ml vancomycin, 2mg/ml amphotericin B, 5% sheep blood, 1.5% trypticase soy agar).

DNA extraction.

Total DNA was extracted from the cecal samples using a commercial kit (DNeasy tissue kit, Qiagen, Germantown, MD) as recommended by the manufacturer except that the cecal samples were digested in the supplied ATL Buffer overnight prior to continuing with the extraction procedure.

T-RFLP analysis.

T-RFLP was performed as outlined previously (11). Briefly, PCR amplification employing primers targeting bacterial 16S rRNA genes (8F and 1492R (101) was performed on each DNA sample (Table 2). The 8F primer was linked to the fluorescent dye 6-FAM (Integrated DNA technologies, Coralville, IA) and the 1492R primer was unlabelled. Each 25 mL PCR reaction contained 20 pmol of each primer, 200 mM of each dNTP, and 1.5 U of *Taq* DNA polymerase in a final concentration of 10 mM Tris-HCl, 50 mM KCl, and 1.5 mM MgCl₂ (Ready To Go PCR beads; Amersham Pharmacia Biotech, Piscataway, NJ).

PCR was performed with the following cycle conditions: initial denaturation at 94°C for 2 min, 30 cycles of denaturation at 94°C for 30s, annealing at 58°C for 45s and extension at 72°C for 90s. A final extension at 72°C for 5 min was performed. The PCR product was purified using GFX purification columns (Amersham Pharmacia Biotech). 200 ng of purified PCR amplicon was cut individually with the restriction enzymes Hhal and Mspl (New England Biolabs, Beverly, MA) for 1-2 hours at 37°C (64). The DNA fragments were separated on an ABI 3100 Genetic Analyzer automated sequence analyzer (Applied Biosystems Instruments, Foster City, CA) in GeneScan mode at Michigan State University's sequencing facility. The 5' terminal restriction fragments (TRFs) were detected by excitation of the 6-FAM molecule attached to the forward primer. The sizes and abundance of the fragments was calculated using GeneScan 3.7. The PCR conditions and the restriction digest conditions were chosen to allow maximal reproducibility.

Analysis of T-RFLP profiles.

Profiles were analyzed as follows using Microsoft Excel and the JMP statistical package. Calculations were performed on profiles generated by digestion of fluorescently labeled PCR amplicons with both *Hha*l and *Msp*l. To standardize each profile for the quantity of labeled DNA present in each sample, the sum of TRF peak heights in each profile being compared was calculated. The sum of peak heights generally varied less than two fold over all of the profiles.

Each sum of TRF peak heights was normalized to the lowest sum of peak heights of the comparison samples. This yielded a correction factor that was applied to each peak in a given profile. The resultant peak heights were filtered to eliminate peaks with a height below the noise threshold (set at a relative fluorescence value of 50).

Additional analysis of T-RFLP was performed in a manner to allow comparison of profiles using standard measures of ecologic diversity. A computer program that uses a statistical method for analysis of multiple T-RFLP profiles was used to group (bin) (1). Once the TRFs were binned a similarity matrix was produced that indicated the relative proportion of each group for each sample.

The Bray-Curtis similarity index was calculated as: $C_N = \frac{2jN}{N_a + N_b}$, where

N_a is the total number of T-RFs in sample A and N_b is the total number of T-RFs in sample B, and 2jN is the sum of the lower of the 2 abundances for the T-RFs found in both samples. This calculation was performed for each pair-wise comparison was calculated by importing the similarity matrix into the program EstimateS (http://viceroy.eeb.uconn.edu/EstimateS). To provide a visual method for the comparison of multiple samples unweighted pair group method with arithmetic mean (UPGMA) trees were constructed using MEGA3 (60).

Calculation of diversity indices.

For each normalized T-RFLP profile, the number and height of peaks in each profile were considered to represent the number and relative abundance of different phylotypes present in the sample. Phylotype richness (S) was calculated as the total number of distinct TRF peaks in each normalized profile. The Shannon-Weiner diversity index was calculated as: $H = -\sum_{i=1}^{i=S} p_i \ln p_i$ where p_i is the proportion of the ith peak relative to the sum of all peak heights. Evenness was calculated as H/H_{max} where $H_{max} = \ln(S)$ (the case when all p_i are equal, therefore $p_i = 1/S$). An additional calculation was preformed for T-RFLP profiles from H. hepaticus-infected animals. In this case, the H. hepaticus-specific TRF was removed from each profile prior to the nomalization procedure and the calculation of diversity indices.

Clone libraries.

The community structure of infected and uninfected mice was also analyzed by the construction of 16S clone libraries. Unlabelled 8F and 1492R primers were used to amplify DNA samples using the same conditions as for T-RFLP analysis. Following purification the PCR products were ligated into a T-tailed plasmid vector (pCR 2.1; Invitrogen, Carlsbad, CA). DNA sequence and sequence analysis were performed as detailed previously (123). Briefly, each clone was sequenced with a single primer (519R) that typically yielded ~500

bases of readable sequence (Table 2). Sequences were analyzed for the formation of chimeras using the Chimera Check program from the Ribosomal Database Project (21). Potential chimeric sequences were excluded from additional analysis. Sequences were aligned to one another using the ARB suite of programs (available through http://www.arb-home.de) Regions of ambiguous alignment (primarily stem structures of variable length) were excluded from the final comparison of sequences such that 342 positions were used in the final phylogenetic analyses. Phylogenetic trees were calculated using the ARB neighbor-joining algorithm.

Grouping of 16S clone library sequences and rarefaction analysis (45) was performed using the FastGroup program (102) available at http://phage.sdsu.edu/research/projects/fastgroup/. Coverage estimations were calculated by the method of Good (43) using the calculation of [1-(n/N)]x100, where n= number of molecular species represented by one clone and N is the total number of sequences in the library.

Statistical differences in the composition of clone libraries from infected and uninfected samples were determined using LIBSHUFF (version 1.2) (103). As was done for the T-RFLP profiles, an additional analysis using LIBSHUFF was performed, this time removing rDNA sequences corresponding to *H. hepaticus* prior to statistical analysis.

In silico terminal restriction fragment length polymorphism analysis.

Terminal restriction fragments using the restriction enzymes *Hha*l and *Msp*l were calculated for each of the 16S rDNA clones using a software tool designed to be integrated into the ARB program suite (93). This in silico T-RFLP analysis tool (TRF-CUT) predicts TRFs based on the ARB-aligned sequences. After deleting sequences homologous to *H. hepaticus*, the predicted TRFs were plotted as a histogram using the DeltaGraph software program (Red Rock Software, Salt Lake City, Utah). A uniform bin size of 5 basepairs was used in generating the histograms.

Nucleotide sequences.

The partial 16S rDNA sequences were deposited in GenBank under the accession numbers AY914179 to

AY914315.

	Number of animals			
	6-week time course		2-week	
	IL-10-/-	IL-10+/+	IL-10-/-	IL-10+/+
Challenge Strain				
Wild-type (3B1)	15	15	5	5
3B1::Tn20 (CDT-)	15	15	5	5
Uninfected •	15	15	5	5
Sacrifice			***************************************	
(days post- challenge)	2, 4, 8, 14, and 42		14	

Table 1. A description of the number of animals used for the 6-week time course and 2 week infection studies.

Primer Name	Sequence 5' - 3'
olMR0086	GTGGGTGCAGTTATTGTCTTCCCG
olMR0087	GCCTTCAGTATAAAAGGGGGACC
olMR0088	CCTGCGTGCAATCCATCTT
8F	AGAGTTTGATCCTGGCTCAG
1492R	GGTTACCTTGTTACGACTT
531R	TACCGCGGCTGCTGGCAC
M13F	CAGTCACGACGTTGTAAAACGACGGC
M13R	CAGGAAACAGCTATGACCATC

Table 2. Primer sequences.

Results

Mouse infections with *H. hepaticus*

H. hepaticus strain 3B1 (the type strain) was administered via oral gavage to four wild type C57BL/6 mice. An equal number of control animals received sterile culture broth. The animals were monitored for colonization with H. hepaticus by culture and H. hepaticus-specific PCR performed on freshly voided fecal pellets. All of the animals infected with H. hepaticus remained colonized with H. hepaticus for the 30-day duration of this experiment (data not shown).

Thirty days after infection with *H. hepaticus*, the animals underwent gastrointestinal necropsy. The cecal tip was harvested and the luminal contents removed. The tissue was longitudinally divided into four sections and frozen for subsequent DNA extraction. None of the animals were found to have gross lesions at necropsy and histologic examination of the cecum and colon did not reveal any typhlocolitis in either the control or infected animals (data not shown).

T-RFLP analysis of cecal tissue 30 days after *H. hepaticus* infection

DNA was extracted from frozen cecal tissue and analyzed by T-RFLP using the restriction enzymes *Hha*l and *Msp*l. To determine the expected location for the *H. hepaticus*-specific terminal restriction fragment (TRF) within a T-RFLP profile, purified genomic DNA from *H. hepaticus* strain 3B1 was also subjected to T-RFLP analysis.

Visual inspection of the T-RFLP traces reveals that infected animals possessed a prominent TRF corresponding to a *H. hepaticus* TRF (Figure 1) whereas profiles from uninfected animals lacked this TRF. To quantify changes in the community structure of mucosal-associated microbiota associated with colonization by *H. hepaticus*, traditional indices of ecologic diversity were calculated for both the *Hha*l and *Msp*l T-RFLP profiles. As seen in Figure 2, colonization with *H. hepaticus* was associated with a significant decrease in both overall diversity (as measured by the Shannon-Weiner diversity index, *H*) and evenness (*H/H_{max}*). There was no significant difference in the number of TRFs encountered in the T-RFLP profiles from infected animals compared to uninfected animals (data not shown).

To determine to what extent the changes in diversity and evenness were due to the dominance that *H. hepaticus* assumed within the community, these indices were recalculated. This time, the *H. hepaticus*-specific TRF was removed from each profile obtained from an infected animal before calculation of the diversity and evenness. When the *H. hepaticus*-specific TRF was suppressed, the differences between the infected animals and uninfected animals was no longer statistically significant (Figure 2).

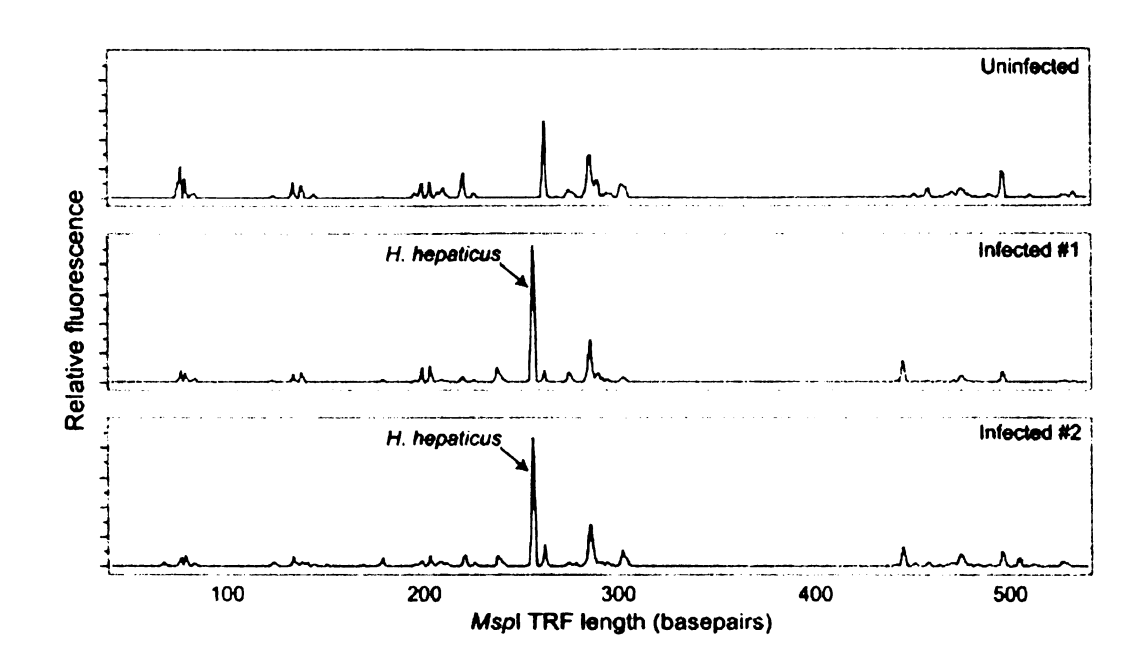


Figure 1. Representative T-RFLP traces comparing the mucosa-associated microbiota in the cecae of an uninfected C57BL/6 mouse and two mice infected with H. hepaticus 30 days previously. The relative fluorescence of each peak is plotted against the size of the peak. In the traces from the two infected animals, a terminal restriction fragment (TRF) corresponding to a H. hepaticus-specific TRF is clearly seen, and is the dominant TRF

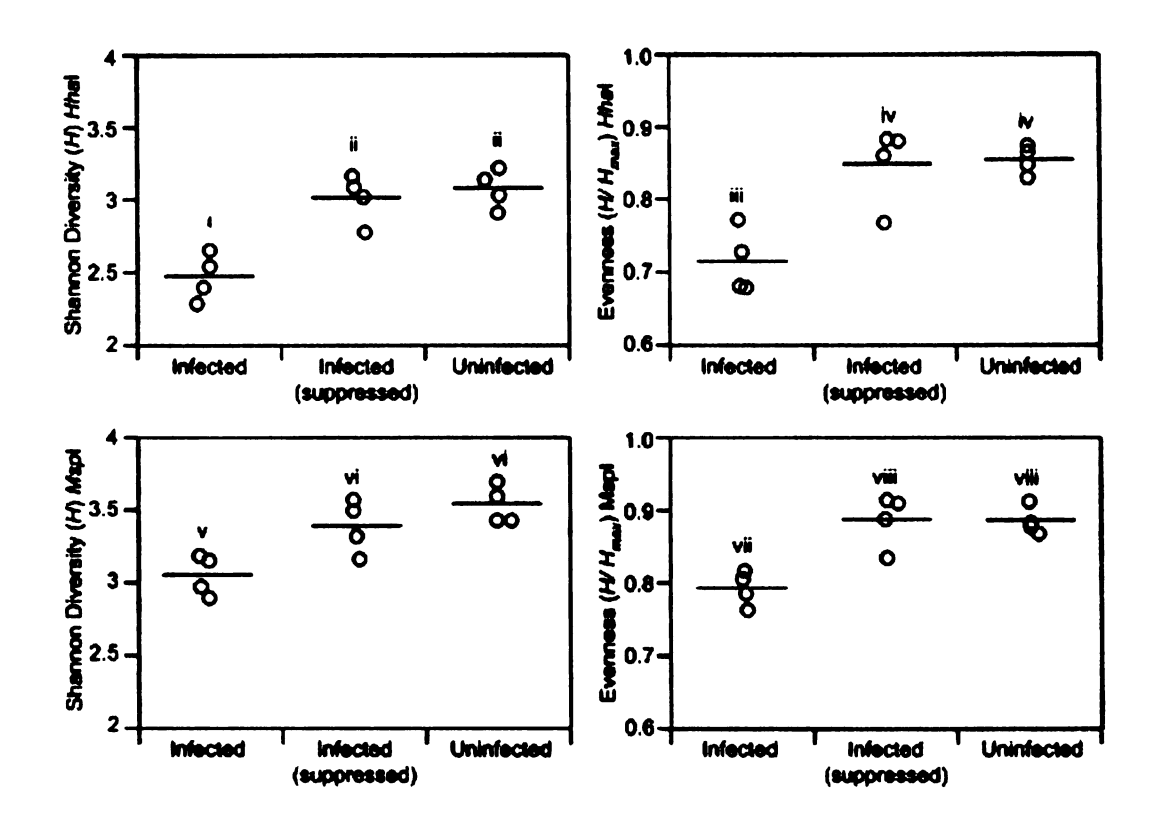


Figure 2. Changes in diversity measures of the mucosal-associated microbiota of the murine cecum 30 days after experimental infection with H. hepaticus. The Shannon Diversity index (H) and Shannon Evenness (H/Hmax) was calculated for each mouse based on normalized T-RFLP profiles obtained with Hhal and Mspl digestion. Compared to uninfected animals (Uninfected category), animals experimentally infected with H. hepaticus (Infected category) had significant decreases in both diversity and evenness. When the analysis was repeated, this time suppressing the H. hepaticus terminal restriction fragment before normalization of the profiles (Infected (suppressed) category), the change in diversity and evenness in infected animals was no longer apparent. Comparisons for all pairs of time points was performed by ANOVA using Tukey-Kramer HSD. Categories within each plot not connected by the same Roman numeral are significantly different with an alpha level set to 0.05

Clone library analysis

T-RFLP analysis provides a relatively inexpensive and high-throughput method for performing microbial community analyses. However, although an overall "fingerprint" of the community is obtained by T-RFLP, it is difficult to identify specific members of the community, unless their presence is suspected beforehand (as is the case with *H. hepaticus* in experimentally infected animals).

To provide insight into the specific bacterial species present in the tissue from *H. hepaticus*-infected and uninfected mice, 16S clone libraries were constructed. 16S sequences were amplified from cecal tissue DNA from a *H. hepaticus*-infected mouse and an uninfected control using the same eubacterial primers used for T-RFLP analysis. The resultant amplicons were cloned into a T-tailed plasmid vector, and the DNA sequence determined for a set of randomly selected clones from each library.

Examination of a phylogenetic tree that combines the 16S sequences obtained from an uninfected animal and an infected animal reveals that *H. hepaticus* 16S sequences were present only in the library from the infected animal (Figure 3). LIBSHUFF analysis (103) indicated that the composition of the two libraries was significantly different when comparing the uninfected library to the infected library, suggesting that the underlying communities being sampled were different. However, if 16S sequences homologous to *H. hepaticus* are deleted from the library constructed from the infected animal prior to LIBSHUFF analysis, this difference is no longer significant (Figure 3).

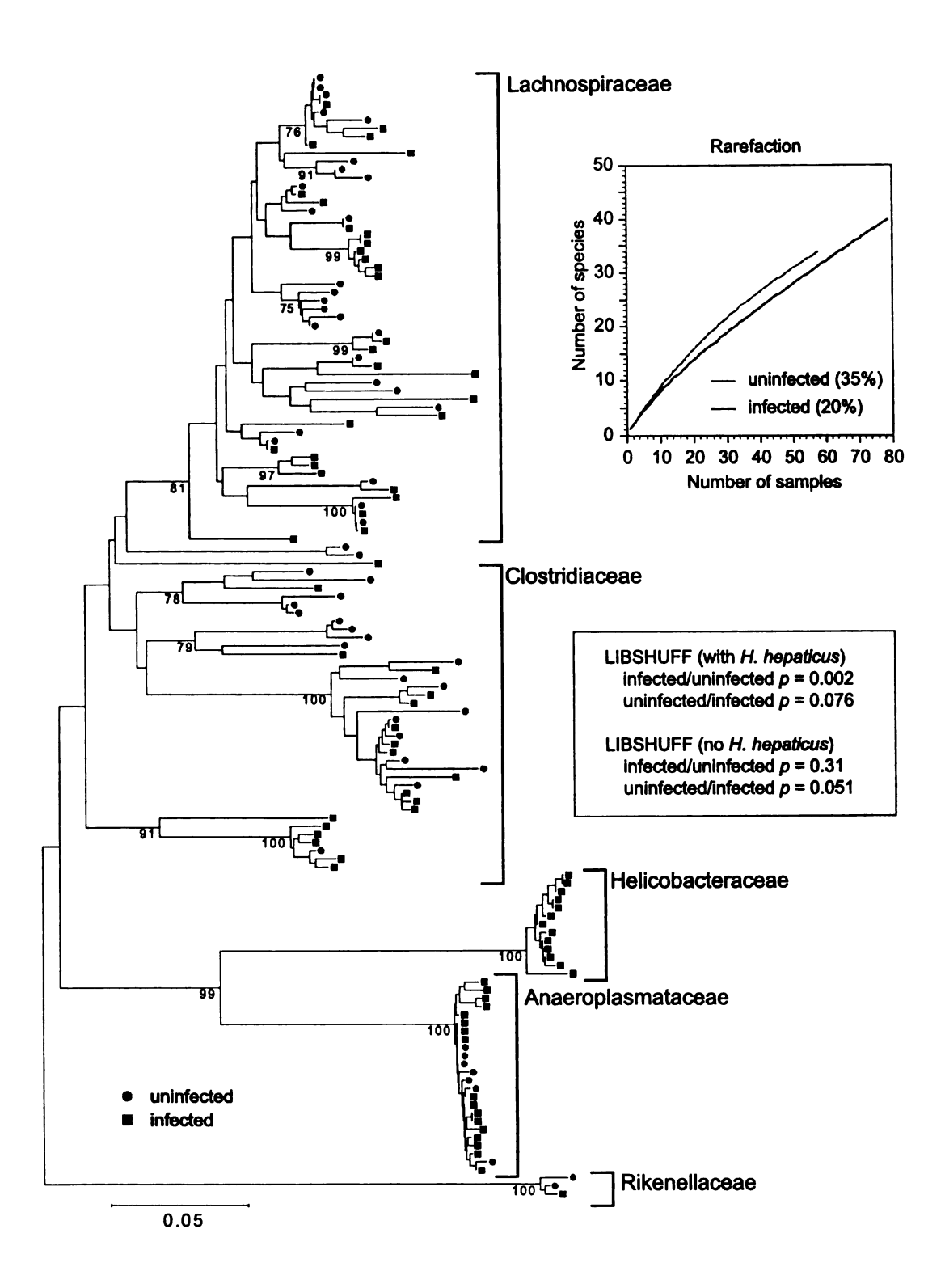


Figure 3. Phylogenetic tree showing the distribution of 16S rDNA sequences from clone libraries constructed from cecal DNA samples obtained from an uninfected mouse (green circles) or a mouse 30 days after infection with *H. hepaticus* (red squares). Brackets outline major clusters of organisms. The scale bar represents evolutionary distance (5 substitutions per 100 nucleotides). The tree was constructed by neighbor-joining analysis using the MEGA program. Analysis was performed on a multiple-sequence alignment generated using the ARB suite of programs. Clones representing *H. hepaticus* were found only in the clone library constructed from DNA from the infected animal. The graph show rarefaction curves for each library long with Good's coverage estimate in parentheses. The results of LIBSHUFF analysis (40) of the two libraries, with and without inclusion of *H. hepaticus* 16S rDNA sequences is shown in the inset.

To compare the community profile obtained by T-RFLP analysis with that provided by clone library analysis, an in silico analysis of the partial 16S rDNA sequences was performed. *Hha*l and *Msp*l TRFs were predicted for each 16S rDNA clone, with the exception of clones homologous to *H. hepaticus*, using an ARB software-integrated tool (93). The in silico-generated TRFs were plotted in histogram format to reflect the number of times a specific in silico TRF was encountered and these plots compared to actual T-RFLP traces from uninfected mice (Figure 4). The plots of the silico generated TRFs were quite similar to the actual T-RFLP traces.

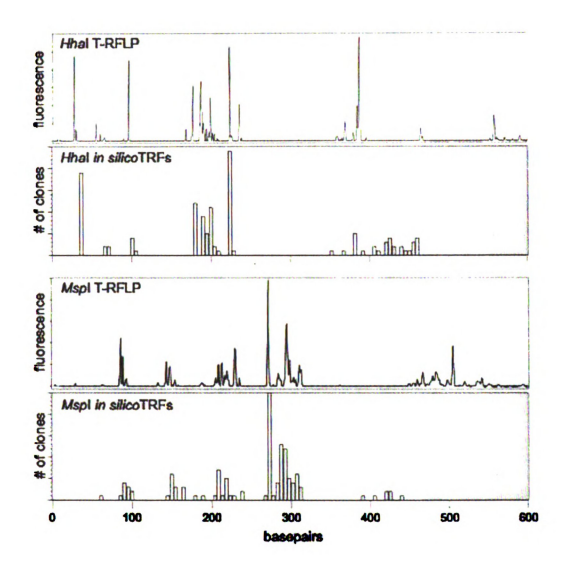


Figure 4. Comparison between T-RFLP analysis and in silico terminal restriction fragment length polymorphism analysis. *Hhal* and *Mspl* TRFs were predicted for each 16S rDNA clone depicted in Figure 3, with the exception of clones homologous to *H. hepaticus*. The in silico-generated TRFs are plotted in histogram format below a corresponding actual T-RFLP trace from an uninfected animal for each enzyme. The grey areas of the histograms above 470 basepairs represents the area where we would not expect to see predicted TRFs given that the maximal length of any given partial 16S sequence was 470 basepairs (see materials and methods).

Time course of infection with wild-type *H. hepaticus* (3B1)

The above results indicate that *H. hepaticus* becomes a dominant member of the cecal mucosa-associated microbiota one month after experimental infection and that *H. hepaticus* colonization results in a decrease in the diversity of the microbiota. In order to follow the dynamics of colonization of the cecal mucosa by *H. hepaticus* a time course experiment was performed. Groups of three C57BL/6 mice were infected with *H. hepaticus* via oral gavage. An equal number of control animals received sterile culture broth. At 2, 8, 14 and 42 days after infection, one experimental and one control group of mice was sacrificed and the cecal tissue taken for histopathology and T-RFLP analysis. As in the 30-day infection experiment, wild type C57BL/6 animals did not develop significant inflammation or hyperplasia in the setting of *H. hepaticus* colonization (data not shown).

Figure 5 shows representative *Msp*l T-RFLP traces from cecal samples of mice at 2, 8, 14 and 42 days after infection with *H. hepaticus*. At all time points, a TRF corresponding to the *H. hepaticus*-specific TRF, was visible in each tracing. This TRF was not seen in any of the uninfected control animals (data not shown).

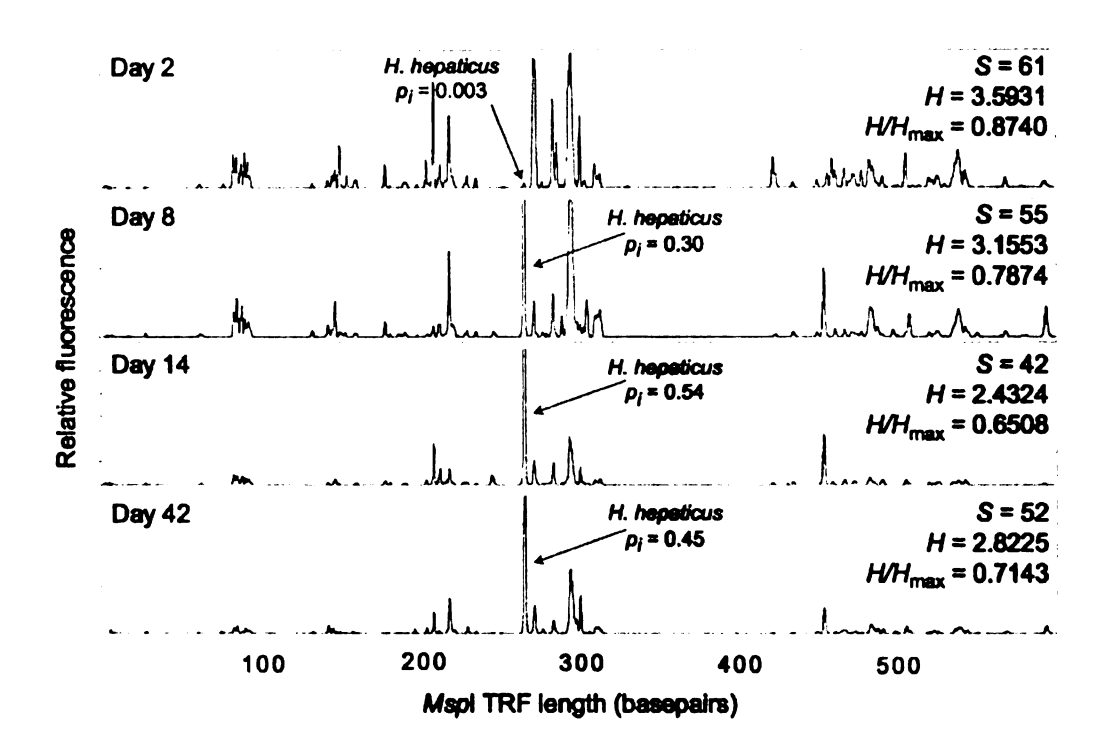
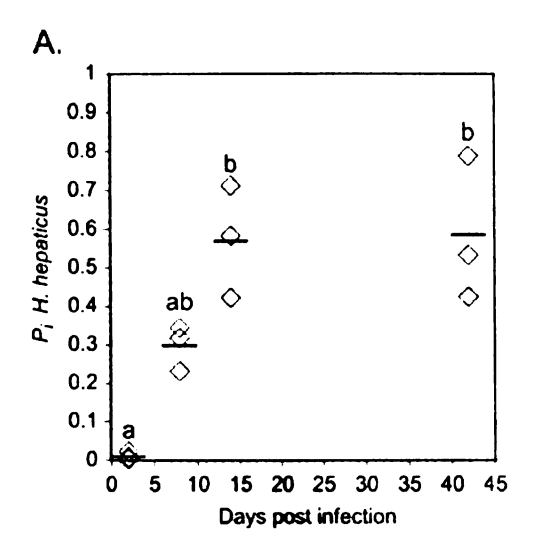


Figure 5. Representative T-RFLP traces temporally monitoring the establishment of colonization in the murine cecum by *H. hepaticus*. Two days after infection, *H. hepaticus* is only a minor fraction (pi) of the total cecal microbiota, but by eight days after infection, is becomes a major component (pi = 0.30) of the total. By 14 days after infection, *H. hepaticus* is the dominant member of the mucosa-associated microbiota, and this dominance persists through 42 days after infection. For each trace, the number of peaks (S), Shannon-Weiner diversity index (H), and Shannon evenness (H/Hmax) is shown

To provide an estimate of the level of colonization by *H. hepaticus* at each time point, the fraction of the total represented by the *H. hepaticus*-specific TRF was calculated. At the earliest time point, the *H. hepaticus* TRF represented only a small fraction (<1%) of the total TRF signal (calculated by peak height) in the tracing. Over time however, the H. hepaticus-specific TRF became the dominant TRF seen, eventually representing ~50% of the total signal in the trace. This result was consistent over all of the animals examined. Figure 6A plots the relative fraction represented by the H. hepaticus-specific TRF in each animal at each time point. The H. hepaticus-specific TRF is initially a minor component of the total community at two days after infection, but becomes a major component at 8 days after infection and the dominant component by 14 days. This predominance of the *H. hepaticus*-specific TRF remained at 42 days after infection. In contrast, there was no change in the appearance of the T-RFLP profiles for the uninfected animals over the entire 42 day time course (data not shown).

A plot of the Shannon-Weiner diversity index during the time course reveals that as *H. hepaticus* becomes increasingly dominant as a component of the mucosa-associated microbiota, the overall diversity of the community decreases (Figure 6B).



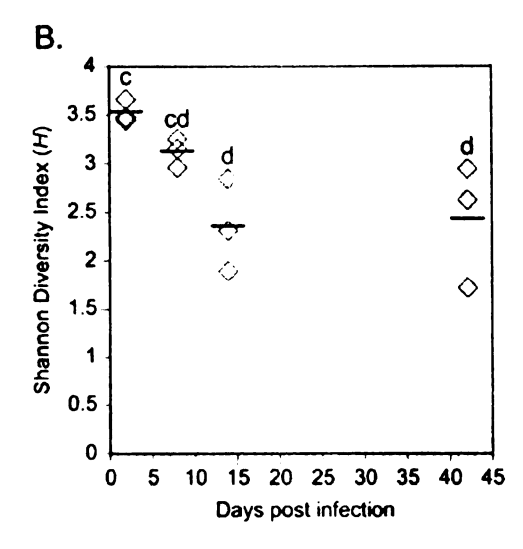


Figure 6. Summary of the temporal monitoring of the colonization of the cecae of mice by *H. hepaticus*. A. The fraction of the total community represented by *H. hepaticus* (*pi*, as calculated by T-RFLP analysis) is plotted for the three mice in each experimental group at 2, 8, 14 and 42 days after infection. *H. hepaticus* is initially a minor component of the mucosa-associated microbiota two days after infection, but by 14 days after infection becomes the predominant member of the community. B. The Shannon Diversity index (H) plotted for the three mice in each experimental group at 2, 8, 14 and 42 days after infection. As the *pi* of *H. hepaticus* increase, this is accompanied by a corresponding decrease in the diversity of the mucosa-associated microbiota. Comparisons for all pairs of time points were performed by ANOVA using Tukey-Kramer HSD. Time points not connected by the same letter are significantly different with an alpha level set to 0.05.

Time course of infection with a CDT- deficient mutant *H.*hepaticus

We have previously shown that infection of IL-10^{-/-} mice with a CDT-deficient *H. hepaticus* mutant is associated with decreased IBD activity six weeks after challenge compared to animals infected with wild-type *H. hepaticus* (121). Both the CDT-deficient mutant and wild-type *H. hepaticus* were detected by culture and PCR in the feces and tissue of all animals at the end of this six-week infection study.

In order to compare the early colonization kinetics of the CDT-deficient mutant to wild-type *H. hepaticus*, a time course infection study was performed. The *H. hepaticus* mutant 3B1::Tn20 is deficient in CDT-production due to a transposon insertion in the *cdtA* gene of the type strain of *H. hepaticus* (121). Groups of three mice were challenged via oral gavage with either wild type *H. hepaticus* or the isogenic CDT-deficient mutant 3B1::Tn20 (121) (Table 1). In a manner analogous to the timecourse with the wild-type *H. hepaticus* detailed above, animals were sacrificed at 2, 4, 8, 14 and 42 days after experimental challenge and the cecal tissue harvested to assess the development of inflammation and to determine relative levels of colonization of the mucosa by *H. hepaticus*.

Animals infected with the CDT-deficient mutant 3B1::Tn20 did not exhibit significant cecal inflammation at any time after challenge (Figure 7). Animals infected with wild-type *H. hepaticus* however, developed histologically significant

typhlocolitis as early as 8 days after challenge (Figure 7). Uninfected control animals did not develop any significant inflammation (data not shown).

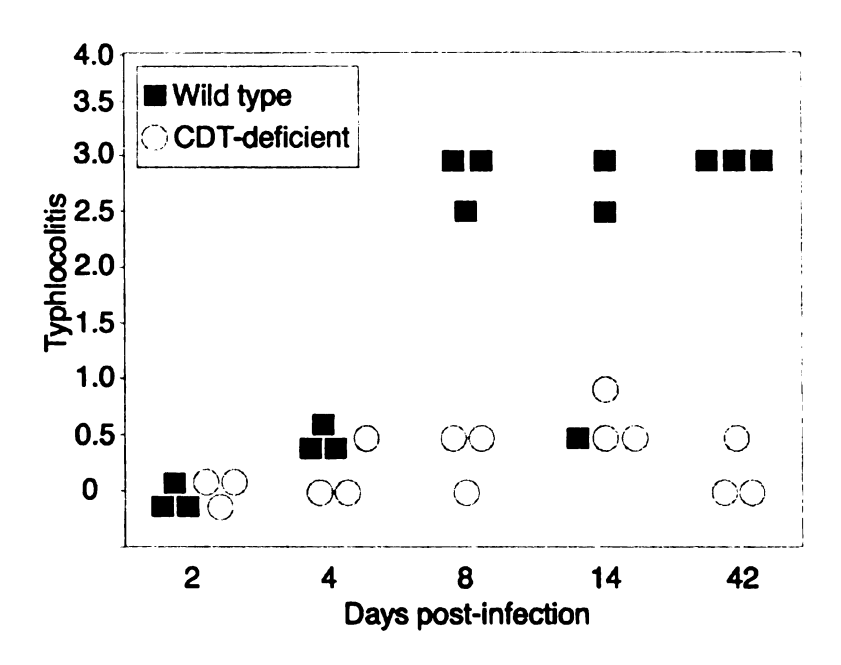


Figure 7. Temporal development of typhlocolitis in IL-10-/- mice infected with wild-type *H. hepaticus* or a CDT-deficient isogenic mutant. Animals infected with wild-type *H. hepaticus* develop severe inflammation within 8 days after experimental challenge, whereas animals infected with the CDT-deficient mutant do not develop significant colitis.

Although all animals challenged with either wild-type H. hepaticus or the CDT-deficient mutant had the organism detectable by culture or *H. hepaticus*specific PCR of feces, we wished to compare the colonization of the cecal mucosa by each isogenic strain. We used T-RFLP analysis to compare the colonization kinetics of wild-type H. hepaticus and the CDT-deficient mutant in the IL-10^{-/-} mice. Wild-type *H. hepaticus* rapidly colonized the cecal mucosa of IL-10^{-/-} mice, comprising approximately 50% of mucosa-associated microbiota by 14 days post-challenge (Figure 8). These are similar kinetics to the colonization of the cecal mucosa of wild-type mice. The CDT-deficient mutant appeared to have somewhat delayed kinetics, not being detectable as a major terminal restriction fragment (TRF) at 8 days after challenge and not becoming the dominant TRF until 42 days after challenge. However, at 42 days, the CDT-deficient mutant was the dominant component of the mucosa-associated microbiota in two of the three mice, and was easily detectable in the remaining animal (Figure 8). Thus the CDT-deficient mutant can still become a significant member of the cecalassociated microbiota, but does so with delayed kinetics compared to wild-type and does not trigger significant typhlocolitis.

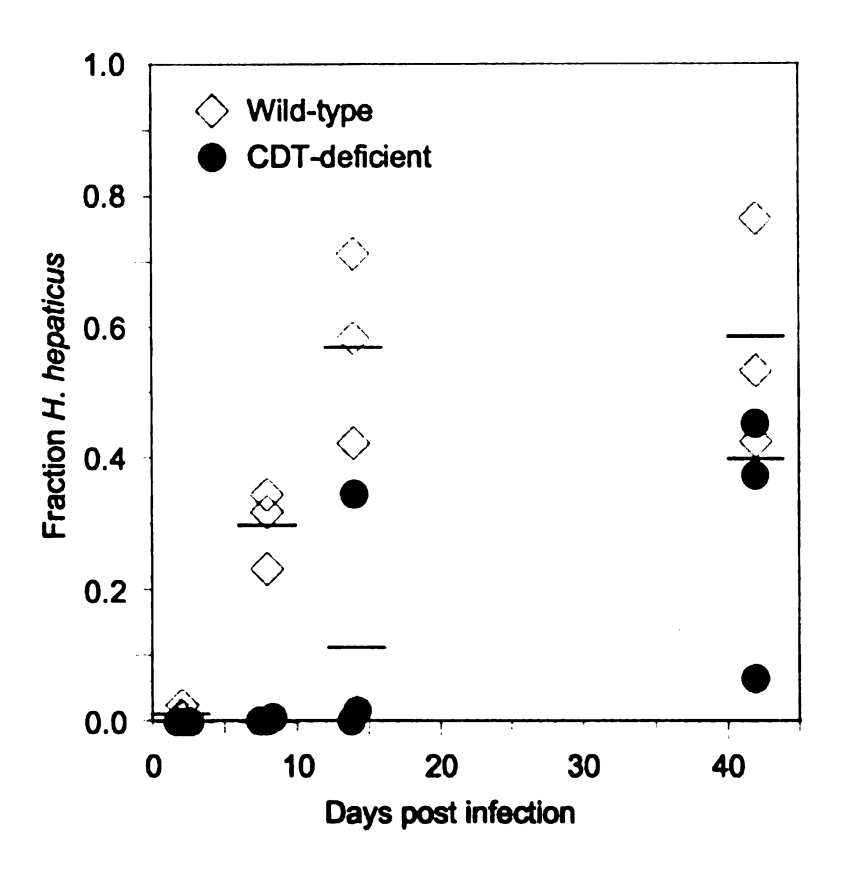


Figure 8. Monitoring the colonization of IL-10-/- mice with *H. hepaticus*. T-RFLP analysis was used to determine the fraction of the mucosa-associated microbiota represented by *H. hepaticus* in animals infected with wild type or the CDT-deficient mutant. The CDT-deficient mutant appears to colonize with slightly delayed kinetic compared to wildtype, but by 42 days after infection, reaches a similar level among the cecal microbiota.

Infection of C57BL/6 IL-10-/- and IL-10+/+ animals with 3B1 (wild-type strain) or 3B1::Tn20 (mutant strain) of *H. hepaticus*.

It has already been established by the previous time course infection studies that at 2 weeks post-infection with the CDT+ wild-type H. hepaticus strain significant inflammation is present whereas, at 2 weeks post-infection with the CDT deficient mutant *H. hepaticus* strain no inflammation is present (Figure 7). IL-10+/+ animals do not get inflammation with the CDT+ or CDT deficient strain of *H. hepaticus*. A new experiment involving a 2-week infection period was conducted in which groups of 4 to 5 mice were divided into experimental groups of: C57BL/6 wild-type mice infected with 3B1 (wild-type strain) or the 3B1::Tn20 (mutant strain) with uninfected controls and C57BL/6 IL-10-/- mice infected with 3B1 (wild-type strain) or the 3B1::Tn20 (mutant strain) with uninfected controls (Table 1). T-RFLP analysis was conducted on all samples using restriction enzyme Mspl. To determine if inflammation has an affect on the diversity of the mucosa-associated microbial community of the gut statistical analysis was conducted with (Figure 9) and without (Figure 10) the TRF associated with H. hepaticus. In both cases of with or without the H. hepaticus TRF the communities from each of the experimental groups generally grouped together, suggesting that inflammation does have an affect on the diversity of the cecal mucosaassociated microbiota (Figures 9 and 10).

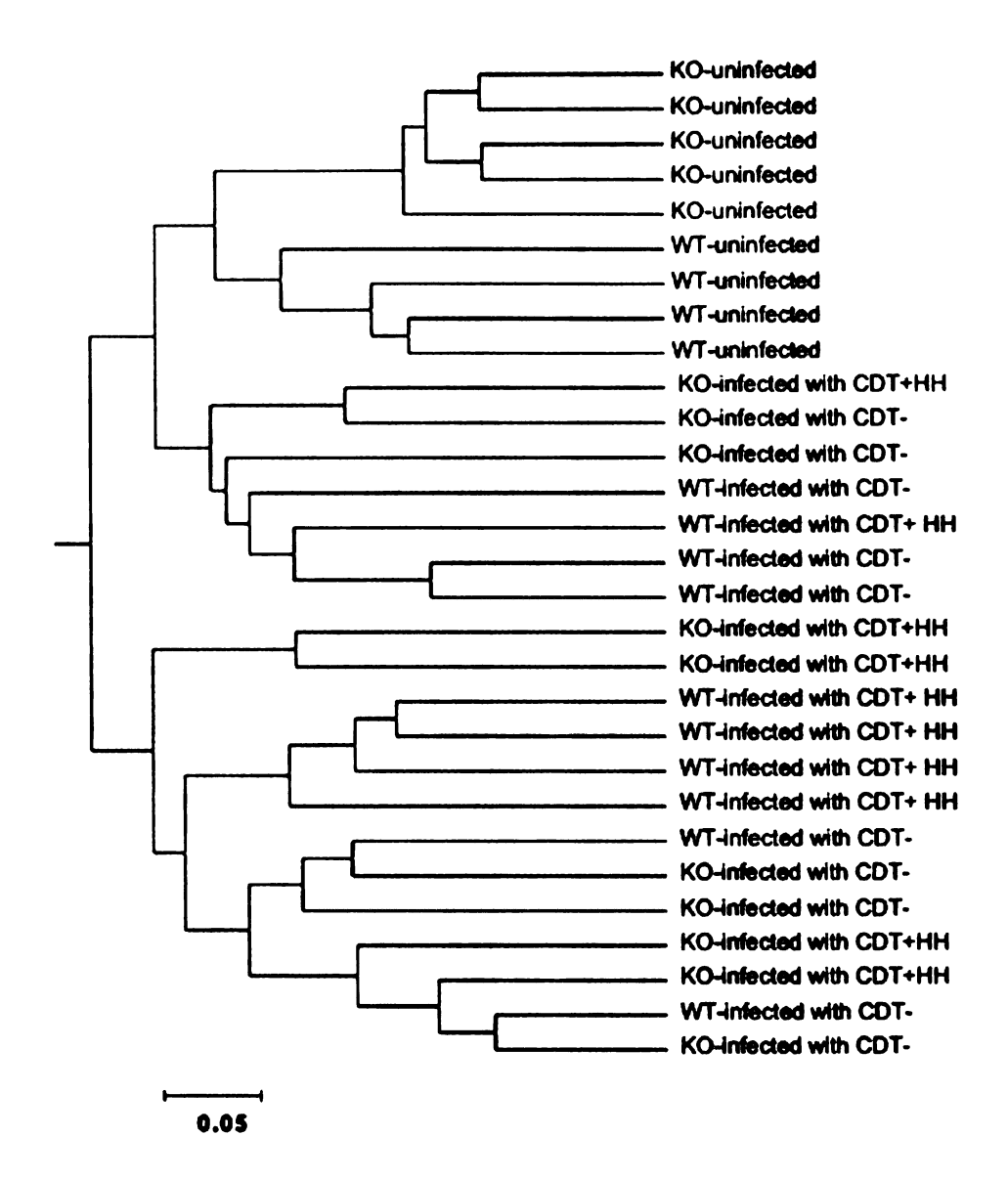


Figure 9. UPGMA dendrogram created using Bray-Curtis distances (1-Bray-Curtis) calculated from T-RFLP analysis of *H. hepaticus* infected versus uninfected KO (IL-10-/-) and WT (IL-10+/+) mice. These animals were either infected with CDT+HH (3B1, *H. hepaticus*) or CDT-HH (3B1::Tn20), *H. hepaticus* CDT deficient mutant). Reproducible changes in the community structure of the mucosa-associated microbiota were detected when comparing the uninfected to the infected animals. Additionally, the mucosa-associated microbiotas of these animals not only group based on the treatment but also by genotype.

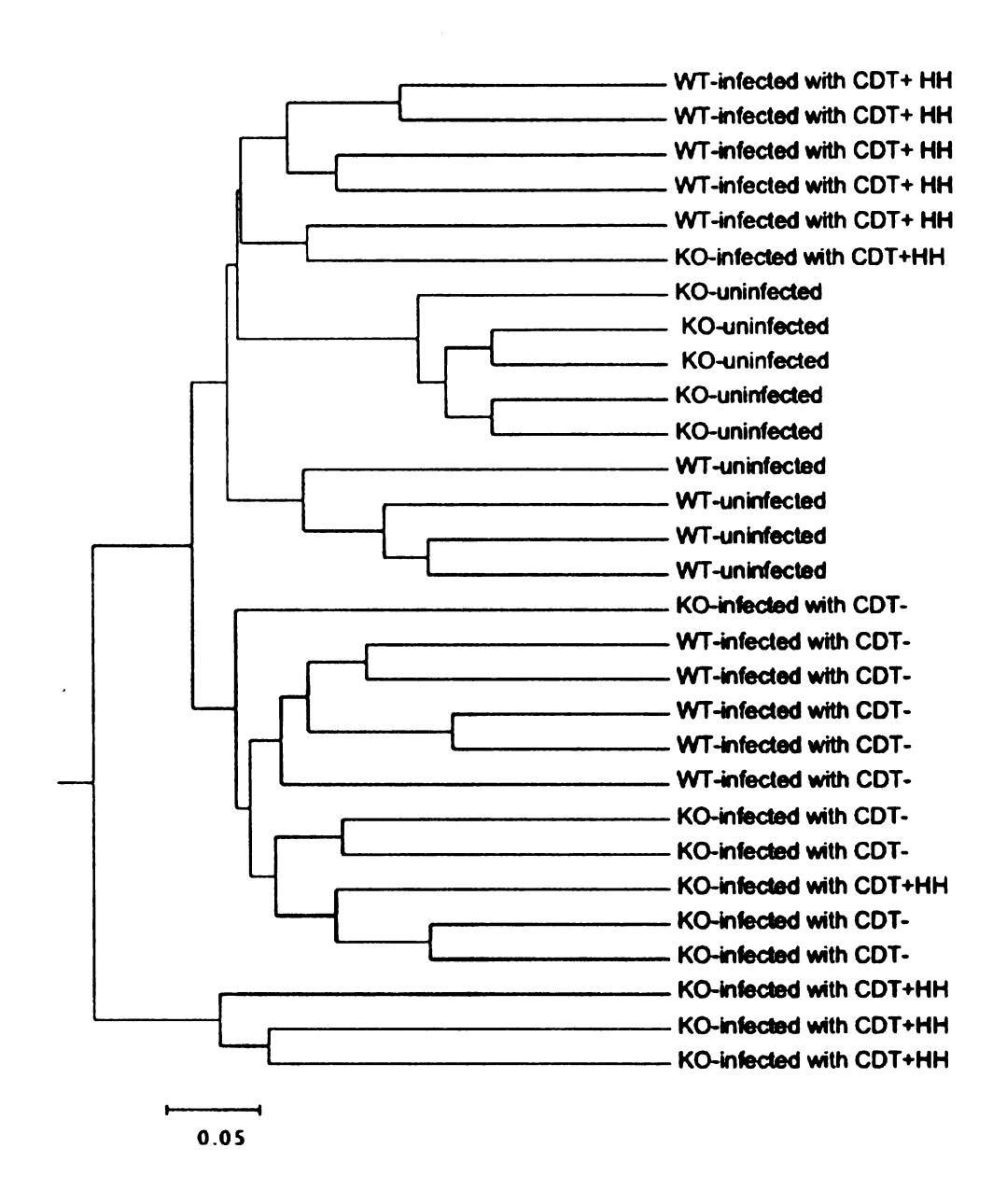


Figure 10. UPGMA dendrogram created using Bray-Curtis distances (1-Bray-Curtis) calculated from T-RFLP analysis of *H. hepaticus* infected versus uninfected KO (IL-10-/-) and WT (IL-10+/+) mice with the *H. hepaticus* TRF removed. These animals were either infected with CDT+HH (3B1, *H. hepaticus*) or CDT-HH (3B1::Tn20, *H. hepaticus* CDT deficient mutant). Reproducible changes in the community structure of the mucosa-associated microbiota were detected when comparing the uninfected to the animals infected with either the CDT+ or CDT- strain of *H. hepaticus*.

Discussion

Colonization is the initial step in the pathogenesis of many enteric bacterial pathogens. A great deal of insight has been gained on the genetic adaptations that enteric pathogens have evolved to permit successful colonization and the eventual development of disease (29, 31). A key emphasis has been placed on examining the interaction between pathogenic bacteria and host cells. An aspect of bacterial pathogenesis that has been less studied is the interaction between pathogenic bacteria and the preexisting microbiota that inhabits a particular ecologic niche within the host. The indigenous microbiota of the host have been postulated to interfere with the invasion pathogenic organisms, so-called "colonization resistance" (12, 36). It has been observed that certain bacteria residing in the GI tract, whether naturally occurring or experimentally administered, can protect the host from pathogenic bacteria (4, 46). It is likely that a number of mechanisms including nutrient depletion, competition for binding sites on the mucosal epithelium and the production of inhibitory substances contribute to colonization resistance (13, 37, 38).

One of the reasons that the interaction between pathogenic bacteria and the indigenous host microbiota has not been studied in detail is that the study of complex microbial communities has been difficult. The intestinal tract of mammals is inhabited by a large and phylogenetically diverse community of microorganisms, many of them obligate anaerobes. Over the past decade, molecular-based approaches have revealed enormous phylogenetic diversity in

the microbial world that is not yet represented in culture (86). These non culture-based techniques, which generally involve the retrieval of the DNA sequence of the small subunit rRNA gene (16S rDNA in the case of bacteria), were initially developed to examine microbial diversity in soil and aquatic environments. More recently, these techniques have been used to examine the indigenous microbiota of mammals. Earlier culture-based examinations of the biota of the mammalian gastrointestinal tract suggested that the majority of morphotypes seen by microscopic examination could be cultivated in the laboratory (77). More recent culture-independent analysis of the microbial ecology of the gastrointestinal tract has suggests that the overall diversity is greater than previously estimated (7, 44, 49, 107, 119). In large part this is due to the fact that sequence-based methodologies can discriminate between bacterial isolates that may have identical morphologies and similar in vitro characteristics.

Initially, culture-independent studies on the mammalian gastrointestinal tract cataloged the species richness that is encountered in that environment (62, 96, 107, 119). More recently, these techniques have also been used to follow changes in the intestinal microbiota over time and to compare the resident microbiota between individuals. These studies have revealed that individuals posses a community of microbes that can vary extensively from individual to individual and within an individual can vary with anatomic location (124). We have used these techniques to follow the changes in the fecal microbiota that can occur in the setting of antibiotic-associated diarrhea (123).

H. hepaticus is a murine pathogen that has been found to be widespread in research mouse colonies. Depending on the strain of mouse, H. hepaticus infection is associated with biliary tract or lower gastrointestinal tract disease. In many strains of mice colonized with H. hepaticus, hepatic disease is subclinical and may be accompanied by subclinical enteritis (generally typhlitis or colitis) (104). However, in mice with altered immune function, the typhlitis/colitis can be severe, leading to rectal prolapse, weight loss and death. This murine typhlitis/colitis in the setting of altered immune function has been employed as a model for inflammatory bowel disease (32).

In the experiments presented here, we used culture-independent community analysis to follow changes in the mucosa-associated microbiota of the cecum during murine infection with *H. hepaticus*. Wild type animals were chosen for the first infection time course infection study to avoid any changes in the microbial community structure secondary to the development of typhlocolitis. In this way, any alterations in the mucosa-associated microbiota could be attributed to colonization by *H. hepaticus* alone, and not by changes in the mucosal environment due to the development of an active inflammatory response.

T-RFLP analysis proved to be a useful method for estimating the abundance of *H. hepaticus* in the mucosa-associated community. Previous studies using culture (35) and a quantitative PCR assay targeting the cytolethal distending toxin of *H. hepaticus* (41), suggest that the organism is encountered in high numbers in the cecum of colonized mice. Although there are potential biases

that result from using PCR to interrogate an entire community (116), the T-RFLP data presented here suggests that *H. hepaticus* becomes the dominant member of the mucosa-associated microbiota of the cecum in infected animals. This conclusion is based on the assumption that peak height by TRF is proportional to abundance of a particular 16S rDNA species in the community, and thus the relative abundance of that particular bacterial species. Clone library analysis also confirmed that *H. hepaticus* readily colonizes the cecal mucosa, and becomes the predominant bacterial species present.

It has been previously suggested that T-RFLP analysis is appropriate for following changes in a given community (56). The use of T-RFLP also revealed that the process of colonization of the cecal mucosa by *H. hepaticus* was associated with reproducible shifts in the overall structure of the microbial community. In the time course experiment, the kinetics by which *H. hepaticus* increased as a component of the community was similar from animal to animal as were the changes in the non-*H. hepaticus* TRFs. Additionally, the C57BL/6 mice in the first experiment came from a different colony than the C57BL/6 mice used in the time course experiment. There were detectable differences in the TRF profiles between uninfected animals from each of these colonies (data not shown). However, the final shifts in the community resulting from *H. hepaticus* colonization were very similar, suggesting that *H. hepaticus* challenge applies a reproducible ecologic stress on the existing microbiota.

We used indices of community diversity, traditionally applied to macroecologic communities such as wetlands and forests, to quantify the changes observed using T-RFLP analysis in the community structure of the mucosa-associated microbiota following colonization with *H. hepaticus*. *H. hepaticus* colonization resulted in a significant decrease in the diversity of this community. This effect appears to be primarily due to the relative dominance that *H. hepaticus* assumes within the community. Reanalysis of the T-RFLP profiles following removal of *H. hepaticus* from the mucosal communities of infected animals revealed that the diversity of the remainder of the community was not significantly different from that seen in uninfected animals. This suggests that *H. hepaticus* has minimal interactions with other members of the indigenous microbiota, at least not interactions detectable by analysis of the entire community by T-RFLP profiling.

Reanalysis of the clone libraries with suppression of *H. hepaticus*-specific clones in general supports the findings of the repeat T-RFLP analysis. However, the finer scale resolution of taxonomic information provided by 16S rDNA sequence analysis supplies some additional insights into the community dynamics encountered in animals infected with *H. hepaticus*. LIBSHUFF analysis provides a measure of the difference between two 16S rDNA clone libraries based on the ability of one library to "cover" the diversity seen in a second library (103). LIBSHUFF analysis of the libraries when *H. hepaticus* 16S rDNA clones are included indicates that the library from the uninfected animal is unable to

provide coverage of the library from the H. hepaticus-infected animal (p = 0.002) but in the reverse case, the library from the infected animal provides at least partial coverage of the library from the uninfected animal (p = 0.076). These results are consistent with the idea that the library from the uninfected animal is a subset of the library from the infected animal (103), and this is supported by visual inspection of the phylogenetic tree. However, repeat LIBSHUFF analysis following the removal of 16S rDNA clones with homology to H. hepaticus provides additional information regarding the diversity of the indigenous microbiota in *H. hepaticus*-infected animals. Repeat analysis shows that the library from the uninfected animal easily provides coverage of the library from the infected animal (p = 0.31) when H. hepaticus is removed. However, there is a trend (p = 0.051) towards inadequate coverage of the library from the uninfected animal by the library from the infected animal. Therefore, while the most obvious changes in diversity, as measured by T-RFLP and clone library analysis, are due to the dominance that H. hepaticus assumes within the community, clone library analysis suggests that more subtle perturbations of the indigenous microbiota may also be occurring.

At first glance it is somewhat surprising that *H. hepaticus* was able to "invade" an established, diverse ecosystem with such ease. However, *H. hepaticus*, a *bona fide* murine pathogen, is excluded from most specific-pathogen free mouse colonies (118). Thus, experimentally introduced *H. hepaticus* may be filling an underutilized or possible "empty" ecologic niche in the gastrointestinal

tract. In part, this can explain the apparent lack of interaction (e.g. direct competition) between *H. hepaticus* and other members of the mucosal microbiota. It has been proposed that successful introduction of an "invasive species" to an established ecosystem is a function of how different an invader is from established species (111).

T-RFLP analysis also revealed that the CDT-deficient mutant has slightly delayed colonization kinetics of the mucosa, but is able to reach comparable levels as those reached by wild-type *H. hepaticus*. These results suggest that CDT production by *H. hepaticus* represents a bacterial adaptation that allows long-term persistence within the mammalian host (121). Fox and colleagues recently reported that CDT expression by *H. hepaticus* is required for long-term colonization of outbred Swiss Webster mice (40). We recently reported that an isogenic *H. hepaticus* mutant that lacked CDT production was able to colonize C57BL/6 IL-10^{-/-} mice, but colonization with the CDT-deficient strain was associated with a significant reduction in IBD activity six weeks after infection compared to animals infected with wild-type *H. hepaticus* (121).

During the separate 2 week infection study, reproducible changes in the community structure of the mucosa-associated microbiota were detected when comparing the uninfected IL-10-/- and IL-10+/+ animals to the animals infected with either the wild-type (CDT+) or the mutant (CDT-) strain of *H. hepaticus*. Interestingly, the microbial communities from the samples were more similar to one another based on treatment and also by genotype, thereby suggesting host

genotype may have an influence on the mucosa-associated microbiota. Studies are being conducted in our lab to determine the effect of host genotype on the composition of the microbiota by analyzing the mucosa-associated microbiota of IL-10-/- and IL-10+/+ raised in the same environment. This is discussed in the next chapter.

The time-course experiments discussed above show that 2 weeks post-infection severe inflammation is observed in the IL-10-/- animals infected with the wild-type CDT+ strain of *H. hepaticus* but not the mutant CDT- strain of *H. hepaticus* do not exhibit inflammation. Together, this suggests that in addition to the factors of introducing a pathogen and host genotype, inflammation also may have an effect the microbial community structure of the mucosa-associated microbiota. Other animal studies support differences are detected in the intestinal microbiota when comparing inflamed versus uninflamed tissue samples (10, 48, 75).

To our knowledge, this is the first time that culture independent techniques have been used to monitor the invasion of a complex mammalian-associated microbial community by a pathogen. Our results demonstrate the power of this type of analysis on revealing details of the relationship between a pathogen and the existing microbiota of the gut. Given the importance of the indigenous GI microbiota in both health and disease, the development and use of methods by which this complex population can be monitored will aid in the study of a wide

variety of gastrointestinal conditions including gastroenteritis, antibioticassociated diarrhea and inflammatory bowel disease.

Chapter 3

The Effect of Host Genotype on the Composition of the Cecal Mucosa-associated Microbiota of Sibling C57BL/6 IL-10+/+ and IL-10-/- Mice

Summary

Experimental infection of specific pathogen free (SPF) C57BL/6 IL-10-/mice by the murine pathogen *H. hepaticus* leads to the development of severe typhlocolitis. Wild-type C57BL/6 mice are stably colonized with H. hepaticus following experimental infection, but develop only minimal disease. Since H. hepaticus appears to trigger typhlocolitis in IL-10-/- animals only in the presence of an established indigenous microbiota, we sought to determine if there were baseline differences in the indigenous microbiota of sibling IL-10+/+ and IL-10-/-C57BL/6 SPF mice. A combination of 16S rRNA-encoding gene clone library analysis and 16S-based terminal restriction fragment length polymorphism (T-RFLP) analysis was used to determine if there are differences in the community structure of the intestinal microbiota due to host genotype. T-RFLP and clone library analysis revealed that at the time of weaning (4 weeks of age) the mucosa-associated microbiota of sibling C57BL/6 IL-10-/- and C57BL/6 wild-type mice was significantly different. At 11 and 19 weeks of age, differences remained, but were somewhat diminished. The differences observed in the sibling IL-10-/- and wild-type mice 16S clone libraries suggest that the status of the host immune system affects the composition of the mucosa-associated microbiota. The differences in the community structure of the mucosa-associated microbiota of the IL-10-/- and wild-type mice, coupled with the significant alterations in the microbiota following H. hepaticus infection could explain the development of severe typhlocolitis in experimentally infected IL-10-/-.

Introduction

Studies report that the mucosa-associated microbiota of individuals with IBD is different than that of normal controls. These differences include a reduction in diversity with loss of beneficial organisms and an increase in mucosa-associated bacteria and invasion (22, 70, 72, 85, 109). It is not clear whether this is due to differences in the microbiota between healthy individuals and those with IBD to begin with or if this difference is due to the disease itself. Human and animal studies have shown that host genotype can influence the composition of the intestinal microbiota (55, 113, 125). Human IBD studies are complicated by the variation seen between individual's microbiota. This variation may be due to differences in environment, diet, genetic background, and disease state. Additionally, to further complicate the issue not all individuals with an immune abnormality (e.g. NOD2 mutation) end up with IBD.

The use of murine IBD models can aid in understanding some of these issues. By using animals from our established C57BL/6 mouse colony of IL-10+/+ and IL-10-/- animals, we can study the microbiota in a controlled environment. We can determine the effect of the host genotype on the composition and diversity of an immune altered host compared to a wild-type host with out disease being a factor (an IL-10-/- animal does not get disease unless infected with *H. hepaticus*). To determine if the host genotype has an effect on the intestinal microbiota a study was conducted in which non-culture based techniques (T-RFLP and clone library analysis) was used to compare the cecal mucosa-

associated microbiota of IL-10+/+, IL-10+/-, and IL-10-/- littermates raised in the same environment.

Materials and Methods

Animals and housing.

A colony of C57BL/6 wild – type and IL-10 -/- mice were housed and maintained in a specific pathogen free environment at Michigan State University. The MSU All University Committee on Animal Use and Care approved all animal protocols used. Food, water and bedding were autoclaved before use. The mice were kept on a 12 – hour light/dark cycle. IL-10-/- and wild-type (IL-10+/+) animals were bred to produce heterozygous (IL-10+/-) animals. These heterozygote animals were subsequently bred with one another to produce litters consisting of wild-type, IL-10-/-, and IL-10+/- animals. A total of three of these litters were produced for this study. The first and second litter originated from the same breeding pair. The first litter was sacrificed at 4 weeks of age. This litter was housed together in the same cage until they were sacrificed. The second litter was sacrificed at 11 weeks of age. The mother of this litter was also sacrificed at this time. These animals were housed together in the same cage until they were weaned. They were then separated by gender for the remaining 7 weeks. The third litter along with the mother was sacrificed at 19 weeks of age. These animals were housed together until they were weaned. They were then separated by sex for the remaining 15 weeks.

Sample collection.

Three litters resulting from the heterozygous crossings were sacrificed for sample collection at varying times. The mice were sacrificed via CO₂ asphyxiation and gastrointestinal necropsy was performed. The cecum was removed by transection of the terminal ileum and the proximal colon. The cecal apex was removed by transection midway down its length at the sharpest point of the curve. The apex was washed thoroughly in 1 X phosphate buffered saline and sectioned longitudinally into three pieces that were snap frozen in a dry ice/ethanol mixture and stored at -80 °C.

DNA extraction.

DNA was extracted from one cecal apex section from each animal using the Qiagen DNeasy tissue kit (Germantown, MD). The manufacturer's instructions were followed with the exception of the 55°C incubation was extended to overnight and the secondary lysis step was extended to 30 min at 70°C.

Genotyping.

Genotyping PCR was carried out following the Jackson Laboratory protocol (http://jaxmice.jax.org/pub-

cgi/protocols.sh?objtype=protocol&protocol_id346) for all animals. GeneAmp

(Applied Biosystems, Foster City, CA) PCR reagents were used and and each 20

μl reaction contained the following: 1X PCR buffer (15 mM Tris-HCl and 50 mM KCl, pH 8.0), 2.5 mM MgCl₂, 0.2 mM dNTPs, 1 μM of each primer olMR0086, olMR0087, and olMR0088, 0.5 U AmpliTaq Gold and 10 ng cecal apex DNA (Table 2). PCR conditions were as follows: denaturation of the DNA template at 94°C for 3 minutes; 35 cycles of 94°C for 30 seconds, 66°C for 45 seconds, 72°C for 45 seconds; with a final extension of 70°C for 2 minutes and the samples were held at 10°C until they were removed. The final PCR products were viewed via a 1.5% agarose gel containing ethidium bromide. The expected results of the PCR: IL-10 +/+, 200 base pair band; IL-10 -/-, 450 base pair band.

Terminal Restriction Length Polymorphism (T-RFLP).

T-RFLP was performed on all DNA samples as previously described (58). The 16S gene was amplified by PCR using the bacterial primers 8F/6-FAM labeled (Integrated DNA technologies, Coralville, IA) and 1492R unlabeled (101) (Table 2). The PCR products were purified using GFX™ (Amersham Phamacia Biotech). The purified PCR products were cut using the restriction enzyme Msp I (New England Biolabs, Beverly, MA). Samples were subjected to capillary electrophoresis using an ABI Prism® 3100 (Applied Biosystems Instruments, Foster City, CA) in Genescan mode. The 6-FAM labeled 8F primer enabled the terminal restriction fragments (T-RFs) to be visualized. GeneScan 3.7 was used to calculate the sizes and abundances of the fragments.

Analysis of T-RFLP profiles.

Analysis of T-RFLP was performed in a manner to allow comparison of profiles using standard measures of ecologic diversity. A computer program that uses a statistical method for analysis of multiple T-RFLP profiles was used to group (bin) (1). Once the TRFs were binned a similarity matrix was produced that indicated the relative proportion of each group for each sample. The Bray-Curtis similarity index was calculated as: $C_N = \frac{2jN}{N_a + N_b}$, where N_a is the total number

of T-RFs in sample A and N_b is the total number of T-RFs in sample B, and 2jN is the sum of the lower of the 2 abundances for the T-RFs found in both samples. This calculation was performed for each pair-wise comparison was calculated by importing the similarity matrix into the program EstimateS (http://viceroy.eeb.uconn.edu/EstimateS). To provide a visual method for the comparison of multiple samples, unweighted pair group method with arithmetic mean (UPGMA) trees were constructed using MEGA3 (60).

Clone libraries.

The 16S gene was amplified by PCR using unlabeled bacterial primers 8F and 1492R(101). The PCR reaction was carried out as stated above in the T-RFLP procedure with the exception of the use of 20 cycles instead of 30 cycles and a 52 °C annealing temperature. The PCR products were purified using GFXTM purification (Amersham Phamacia Biotech). The resulting PCR product

was ligated into the pCR 2.1 TOPO cloning vector (Invitrogen, Carlsbad, CA). Ninety – six white colonies were selected from each library and grown in 96 deep well plates containing LB freezing broth containing 4% v/v glycerol and carbenicillin (50µg/ml) overnight at 37°C. A screening PCR was performed using M13 forward and reverse primers (Table 2). PCR of the cloned product was carried out using Invitrogen reagents (Invitrogen, Carlsbad, CA). Each 25µl reaction contained (1.5 μ l of the *E. coli* overnight growth, 80 μ M of a dNTP mixture, 100 fmol of each M13 primer, 1U of Taq DNA polymerase in a final concentration of 20 mM Tris-HCl, 50 mM KCl, and 1mM MgCl₂). Initial denaturation of DNA template was carried out at 95°C for 5 minutes this was followed by 30 cycles of 95°C for 30 seconds, 55°C for 1 minute, 72°C for 3 minutes; with a final extension of 70°C for 10 minutes. The PCR amplicons were quality checked using E-GEL® 96 (Invitrogen, Carlsbad, CA). The amplicons of the correct size of approximately 1500 bps were processed by ExoSAP-IT (USB Corporation, Cleveland, OH). Each ExoSAP-IT reaction contained (0.25 μ l ExoSAP-IT, 3.25 μ I sterile water, and 1.5 μ I of M13 PCR product). The reactions were incubated for 30 minutes at 37 °C followed by 80 °C for 15 minutes. The processed M13 PCR products were submitted to the Research Technology Support Facility (RTSF) at Michigan State University for sequencing using either the 531R or 8F primers (Table 2).

The raw sequence data were processed through an automated "information pipeline" Ribosomal Database Project (RDP) (rdp.cme.msu.edu).

Through this pipeline the sequences were quality scored, trimmed, and the vector sequence was removed. The resulting trimmed sequences were subjected to secondary alignment and a RNA distance matrix was produced. This RNA distance matrix was imported into DOTUR and EstimateS to calculate standard ecological diversity measurements Shannon-Weiner to compare overall diversity (richness and evenness) within and between communities (99). The Shannon-

Weiner diversity index was calculated as: $H = -\sum_{i=1}^{i=S} p_i \ln p_i$ where p_i is the

proportion of the *i*th sequence relative to the sum of all sequences. Coverage estimations were calculated by the method of Good (43) using the calculation of [1-(n/N)]x100, where n= number of molecular species represented by one clone and N is the total number of sequences in the library.

Statistical differences in the compositions of clone libraries from the IL-10-/-, IL-10+/-, and IL-10+/+ samples were determined using \(\)-LIBSHUFF (http://www.plantpath.wisc.edu/joh/s-libshuff.html) (100). The percent proportion of the sequences classified into phyla by the Ribosomal Database Project Library Compare (Libcompare) for each of the clone libraries (http://rdp.cme.msu.edu).

Results

T-RFLP.

To determine the effect of host genotype on the composition of the cecal mucosa-associated microbiota. T-RFLP was performed on samples from sibling IL-10-/-, IL-10+/+, and IL-10-/+. IL-10 -/- and IL-10+/+ mice were bred to produce litters of mice heterozygous for the IL-10 gene. Two pairs of the resulting heterozygous mice were then bred to produce litters consisting of IL-10 -/-, IL-10+/+, and IL-10+/- mice. Three litters resulting from the heterozygous crossings were sacrificed for sample collection at varying times. The first and second litter originated from the same breeding pair. The first litter containing 5 offspring, was sacrificed at 4 weeks of age. The second litter containing 9 offspring, was sacrificed at 11 weeks of age. The mother of this litter was also sacrificed at this time. The third litter containing 12 offspring were sacrificed along with the mother was sacrificed at 19 weeks of age. Gastrointestinal necropsy was performed at each time point in which the cecal tip was taken and cleared of luminal contents. The cecal tissue was transected longitudinally into three sections and snap frozen for DNA extraction. DNA extraction was performed on frozen tissue and analyzed via T-RFLP using restriction enzyme Mspl. To determine the similarities and differences among cecal mucosa-associated community structures of the IL-10+/+, IL-10-/-, and IL-10+/- animals raised in the same environment statistical analysis was performed using analytical tools from IBEST website (1). An

UPGMA dendrogram was produced using the 1-Bray-Curtis (distance measurement) (Figure 11).

At the time of weaning (4 weeks of age) the mucosa-associated microbiota of sibling IL-10-/- and IL-10+/+ mice were significantly different. At 11 and 19 weeks of age, differences remained, but were not as obvious. The samples from the animals at varying ages are more similar to one another by age demonstrating the mucosa-associated microbial communities from animals of the same age are more similar to one another. The mucosa-associated microbial community from the mother of the 4 and 11 week-old litters is more similar to the 11 week-old animals. Additionally, the mother of the 19 week-old litter is grouped with its litter. Reproducibility of this method was attempted by conducing T-RFLP analysis on two cecal tip sections (a and b) from one animal. This was done with two IL-10-/+ animals (HETa1, b1-11wk-F and HETa2, b2-11 wk-F). The microbial communities from the two cecal tips from each animal did not necessarily group together with the appropriate animal in the dendrogram (Figure 11).

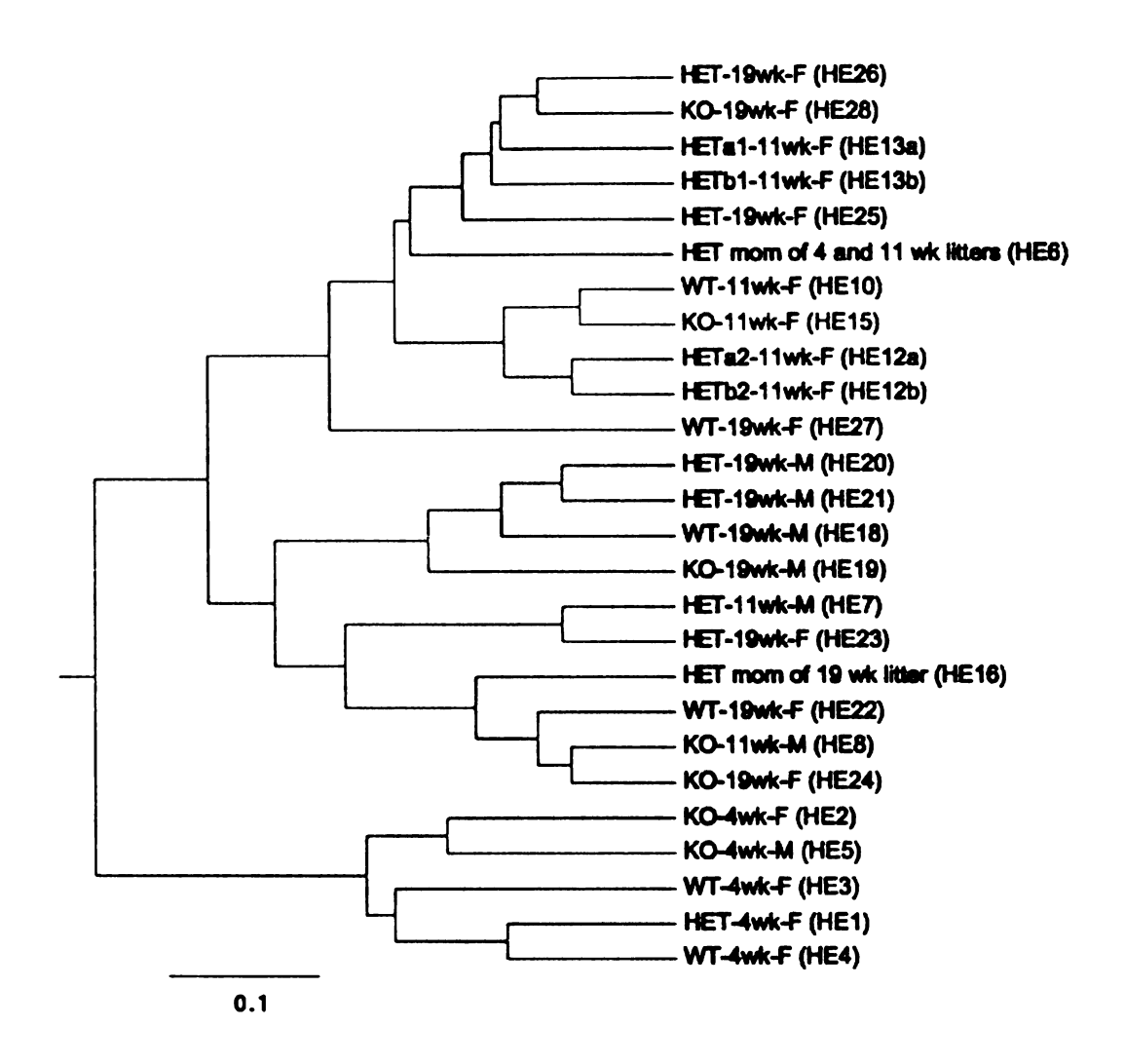


Figure 11. UPGMA dendrogram created using Bray-Curtis distances calculated from T-RFLP analysis of (KO) IL-10-/-, (WT) IL-10+/+, and (HET) IL-10-/+ littermates and their mothers. At the time of weaning (4 weeks of age) the mucosa-associated microbiota of sibling IL-10-/- and IL-10+/+ are significantly different as measured by the Bray-Curtis similarity index. Additionally the mucosa-associated microbiota of IL-10-/+ mouse is more similar to IL-10+/+ mice than to the IL-10-/- mice. At 11 and 19 weeks of age these differences remained but were somewhat diminished. The samples from the animals at varying ages tend to group by age demonstrating the mucosa-associated microbial communities from animals of the same age are more similar to one another. The mucosa-associated microbial community from the mother of the 4 and 11 week old litters is more similar to the 11 week old animals.

Clone library analysis.

Clone library analysis was also performed to examine the community structures of the sibling IL-10+/+ and IL-10-/-. The same bacterial primers used for T-RFLP analysis were used to amplify the 16S rRNA genes using DNA from the cecal tissue of the IL-10-/- and IL-10+/+ animals. The resultant PCR products were cloned into a T-tailed plasmid vector, and the DNA sequence was determined for a set of randomly selected clones from each library. These sequences were processed through an automated "information pipeline" Ribosomal Database Project (RDP) (rdp.cme.msu.edu). UPGMA trees were constructed using the distance measurement (1-Bray-Curtis) (Figure 12). As with the T-RFLP data the clone libraries from the 4 week-old sibling IL-10-/- and IL-10+/+ mice were significantly different, however at the later time points of 11 and 19 weeks of age these differences were not as apparent.

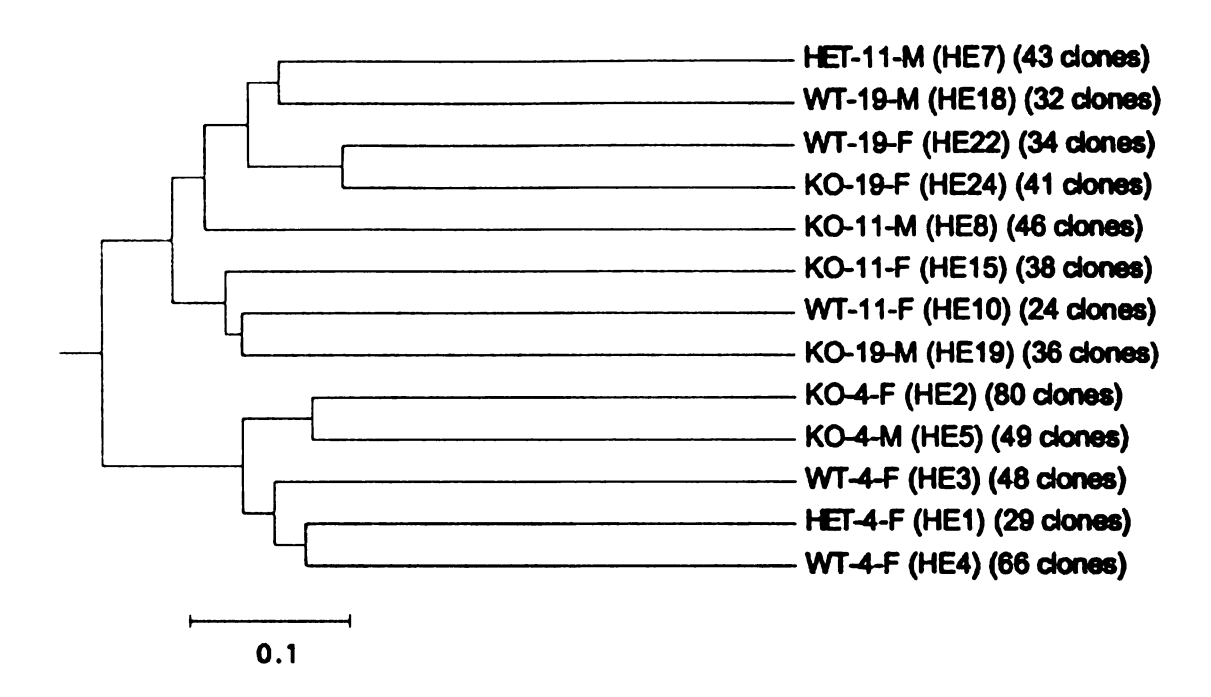


Figure 12. UPGMA dendrogram created using Bray-Curtis distances calculated from clone library analysis of IL-10-/-, IL-10+/+, and IL-10-/+ littermates. The number of clones having sequences greater than 350 base pairs is listed next to each library. At the time of weaning (4 weeks of age) the mucosa-associated microbiota of sibling IL-10-/- and IL-10+/+ are significantly different as measured by the Bray-Curtis similarity index. Additionally the mucosa-associated microbiota of IL-10-/+ mouse is more similar to IL-10+/+ mice than to the IL-10-/-mice. At 11 and 19 weeks of age differences remained but were somewhat diminished.

Table 3 shows for each sample the number of clones, number of OTUs, coverage. Shannon-Weiner diversity index. There was no statistical difference in overall diversity, measured by Shannon-Weiner diversity index, between the microbial communities from the IL-10-/-, IL-10-/+, and IL-10+/+ mice at the different ages using ANOVA (analysis of variance) t- test. Table 4 shows the percent proportion of the sequences classified into Bacteriodetes and Firmicutes for each of the samples. There was no statistical difference in the Firmicutes/Bacteriodetes ratios between the microbial communities from the IL-10-/-, IL-10-/+, and IL-10+/+ mice at the different ages using ANOVA t- test. Statistical differences in the compositions of the clone libraries from the sibling IL-10-/- and IL-10+/+ mice at varying time points was determined using ∫-LIBSHUFF (100) (Table 5). In most cases, libraries from the IL-10+/+ animals are subsets of libraries from the IL-10-/- animals at all ages. The IL-10+/- libraries are more similar to the IL-10+/+ than to the IL-10-/-. Sex appears to have an influence on the composition of the microbiota. With the animals of the same genotype the libraries from the female animals are a subset of the libraries from the male animals. In most comparisons the later time points of libraries from the 11 and 19 week-old animals are subsets of the libraries from the 4 week old animals.

	1		[
			#OTUs		Shannon-
Sample	Description	# of clones	(97%)	Coverage	Weiner
HE001	HET-4-F	29	13	48.28	2.24
HE003	WT-4-F	66	24	71.21	2.65
HE004	WT-4-F	48	26	64.58	3.05
HE002	KO-4-F	80	43	61.25	3.58
HE005	KO-4-M	49	29	51.02	3.12
HE007	HET-11-M	43	28	37.21	3.16
HE010	WT-11-F	24	19	4.17	2.87
HE008	KO-11-M	46	25	65.22	3.01
HE015	KO-11-F	38	24	57.89	3.07
HE022	WT-19-F	34	21	35.29	2.85
HE018	WT-19-M	32	22	40.63	2.99
HE019	KO-19-M	36	24	55.56	3.07
HE024	KO-19-F	41	23	58.54	2.93

Table 3. Diversity statistics for each of the clone libraries from IL-10-/-, IL-10+/-, and IL-10+/+ at 4, 11, and 19 weeks of age.

Phyla

		Sample	Bacteroidetes	Firmicutes	Firmicutes/Bacteroidetes ratio
H	HE001	HET-4-F	10.7	89.3	8.3
H	HE003	WT-4-F	23.4	76.6	3.3
	HE004	WT-4-F	23.4	76.6	3.3
	1E002	KO-4-F	11.4	88.6	7.8
우다	1E005	KO-4-M	6.7	93.3	14.0
ğ	HE007	HET-11-M	20.9	79.1	3.8
<u>ي</u> ق	HE010	WT-11-F	12.5	87.5	7.0
⊃ [;	1E008	KO-11-M	8.7	91.3	10.5
⊕ [i	HE015	KO-11-F	18.4	81.6	4.4
운[HE022	WT-19-M	16.1	83.9	5.2
	HE018	WT-19-F	18.8	81.3	4.3
ω F	HE019	KO-19-M	11.8	88.2	7.5
	HE024	KO-19-F	15.0	85.0	5.7

Table 4. The percent proportion of the sequences that were classified into phyla by the Ribosomal Database Project Libcompare for each of the IL-10-/-, IL-10+/-, and IL-10+/+ samples at 4, 11, and 19 weeks of age.

								>						
		HE001	HE002	HE003	HE004	HE005	HE007	HE008	HE010	HE015	HE018	HE019	HE022	HE024
		HET-4-F KO-4-F			WT-4-F	WT-4-F WT-4-F KO-4-M	HET-11-M KO-11-M WT-11-F KO-11-F WT-19-M KO-10-M	KO-11-M	WT-11-F	KO-11-F	WT-19-M		WT-19-FWT-19-F	WT-19-F
HE001	HET-4-F	0	0.5132	0.311	0.721	0.1906	0.7737	0.0204	0.1679	0.375	0.0093	0.0036	0.1189	0.2773
HE002	KO-4-F	0.2845	0	0.011	0.034	0.7119	0.0056	0	0.7367	0.3895	0.0018	0.0052	0.8027	0.3617
HE003	WT-4-F	0.7709	0.8674	0	0.392	0.0744	0.0812	0	0.0199	0.0214	0.0004	0.0006	0.1595	0.2011
HE004	WT-4-F	0.0138	0.9919	0.177	0	0.0025	0.0023	0	0.2026	0.0234	0.0007	0.0003	0.1699	0.0064
HE005	KO-4-M	0.7424	0.0824	0.258	0.03	0	0.0099	0.003	0.3191	0.1717	0.0213	0.0081	0.1965	0.1318
1E007	HET-11-M	0.1094	0.7502	0.323	0.44	0.0265	0	0.7424	0.7749	0.1232	0.2188	0.326	0.0949	0.0682
HE008	KO-11-M	0	0.0031	0	0	0	0,012	0	0.001	0.0028	0.0007	0.0001	0.0272	0.2416
4E010	WT-11-F	0.6056	0.8113	0.958	0.74	0.9452	0.7582	0.0087	0	0.9798	0.5366	0.7527	0.477	0.4917
4E015	HE015 KO-11-F	0.074	0.9584	0.266	0.061	0.8617	0.1671	0.0014	0.0144	0	0.0011	0.0358	0.0731	0.8807
1E018	HE018 WT-19-M	0.0069	0.9476	0.185	0.227	0.0428	0.7663	0.0882	0.0507	0.0581	0	0.1284	0.8139	0.7096
1E019	HE019 KO-19-M	0.0104	0.9043	0.03	0	0.0072	0.0792	0.0015	0.1754	0.1724	0.0432	0	0.034	0.1967
1E022	HE022 WT-19-F	0.0627	0.853	0.499	0.484	0.3266	0.57	0.0478	0.0973	0.0756	0.1221	0.0186	0	0.2057
HE024	HE024 WT-19-F	2060.0	0.8335	0.169	0.151	0.0952	0.383	0.4498	O COSOR	0 2105	0.0148	0.0844	0 535	O SPECIAL PROPERTY.

10+/4, and IL-10-/4 littermates at 4, 11 and 19 weeks of age. P values are shown for all coverage comparisons. Multiple comparisons were made therefore the Bonferonni correction was performed along with the calculation of the Monte Carlo Table 5. S-LIBSHUFF was used to make all pair-wse comparison between the 13 clone libraries from the IL-10-/-, ILerror. The generated a minimum P value= 0.0003.

Discussion

Studies have demonstrated host genotype affects the composition of the microbiota (63, 113, 125). Differences have been observed in the intestinal microbiota when comparing samples from individuals with IBD versus healthy controls (57, 72, 79, 85, 90). However, it is unknown whether these differences are due to host genotype or the disease itself. Studies have also shown that there are marked differences observed in the intestinal microbiota of individuals due to differences in environment, diet, age, and disease state (53, 78). Human studies are complicated by these variations seen between individuals therefore animal models are commonly used to study the effects of different factors dynamics of the intestinal microbiota.

One such model is a murine IBD model, a C57BL/6 IL-10-/- mouse infected with *Helicobacter Hepaticus*, an enterohepatic murine pathogen.

Introducing *H. hepaticus* into the gut microbiota of a C57BL/6 IL-10-/- mouse elicits an exaggerated Th1 response leading to severe typhilitis/colitis. IL-10 is an important anti-inflammatory cytokine involved in innate and adaptive immunity.

This murine model is commonly employed as a Crohn's disease model. When an IL-10-/- mouse is raised in a specific pathogen free environment it remains disease free. Introduction of *H. hepaticus* into a C57BL/6 IL-10+/+ mouse does not result in disease. We have previously shown that the introduction of *H. hepaticus* into an IL-10+/+ mouse causes measurable perturbations in the microbiota (58). A question that arose from these observations was; why do IL-

10-/- and IL-10+/+ mice react differently to the introduction of *H. hepaticus*? We sought to answer this question by utilizing non-culture based techniques to examine the cecal mucosa-associated microbiota of sibling IL-10-/- and IL-10+/+ mice generated by heterozygous parents. Three litters of varying ages (4, 11 and 19 weeks of age) were used for this study.

The T-RFLP data results show that at 4 weeks of age there are differences seen between IL-10-/- and IL-10+/+ animals however at the later ages these differences did not remain. At the time of weaning (4 weeks of age), the microbial communities could be grouped by the genotype of the mouse. With increasing age, these differences were less apparent, perhaps reflecting a greater influence of diet or the loss of the effect of breast milk on the on community composition. The microbial communities from the IL-10-/+ mice were more similar to the microbial communities from the IL-10+/+ mice than the IL-10-/- mice, perhaps because IL-10 is still present in the IL-10-/+ mice. The samples from the animals at varying ages tend to group by age demonstrating the mucosa-associated microbial communities from animals of the same age are more similar to one another. This may reflect the changes that occur over time when the microbiota is being established. The mucosa-associated microbial community from the mother of the 4 and 11-week-old litters is more similar to the 11-week-old animals. Additionally, the mother of the 19-week-old litter is grouped with its litter. This is not too surprising considering the input microbiota for each of the litters came from their mothers and the microbial communities from the 4

week old animals was distinctly different from the microbial communities from the older animals. Similar results were observed in C57BL/6 mice of 4 to 10 weeks age (56). In Kibe et al. (2004) they conducted T-RFLP on the cecal contents of 4 to 10 week old, female, C57BL/6 mice raised in a specific pathogen environment (56). Using T-RFLP they found that the microbial communities from the 4 week old animals were more similar to one another than the older animals. Similarly, this was also seen with the microbial communities of the10 week old animals (56). However, the microbial communities from the 5 to 8 week old animals were not distinguishable from one another (56). Another study conducted by Ley et al. (2005) found that the intestinal microbial communities of different litters grouped together along with their mothers (63).

Clone libraries were constructed on a subset of the animals at each time point. Statistical differences in the compositions of the clone libraries from the sibling IL-10-/- and IL-10+/+ mice at varying time points was determined using *f*-LIBSHUFF (100) A small P value for ΔC(xy) coupled with a high P value for ΔC(yx) indicates sequences in Y are a sub-sample of sequences in X(100). In most cases, libraries from the IL-10+/+ animals are subsets of libraries from the IL-10-/- animals at all ages thereby, suggesting less restriction on composition. The IL-10+/- libraries are more similar to the IL-10+/+ than to the IL-10-/-. Sex appears to have an influence on the composition of the microbiota. With the animals of the same genotype the libraries from the female animals are a subset of the libraries from the male animals. In most comparisons the later time points

of libraries from the 11 and 19 week-old animals are subsets of the libraries from the 4 week old animals suggesting that at 4 weeks perhaps less restriction on the composition of the microbiota.

The relationships of the microbial communities of the 4 week old animals observed were the same for both the clone library analysis and the T-RFLP analysis suggesting that these relationships are "real". However, the relationships don't necessarily hold true for the animals at the later time points. This could be because there are more strict influences on the composition of the microbiota while it is being established. However, these conclusions cannot be drawn from the clone library data presented here. This is primarily due to the overall low coverage values for the clone libraries. Ideally to make comparisons amongst samples it is best to have equal and complete coverage.

Overall the results from this preliminary study suggest that at the earlier age of 4 weeks distinct differences are observed when comparing the microbial communities from IL-10-/- and IL-10+/+ animals. This study also demonstrates the usefulness of the non-culture based techniques of T-RFLP and 16S clone library analysis with associated computer programs that enable one to compare microbial communities to one another using diversity measurements. T-RFLP, a less expensive high throughput method, is particularly useful when conducting preliminary experiments in which microbial communities from many animals are being compared.

Chapter 4

The Effect of Antibiotic Treatment on the Cecal Mucosa-Associated Microbiota of C57BL/6 Interleukin-10 knockout

Mice

Summary

Crohn's patients have a Th1 exaggerated immune response to their own intestinal microbiota and IBD develops in the areas of highest bacterial concentration, thus incriminating the microbiota in the initiation of disease. Studies show there are differences in the mucosa-associated bacteria in IBD patients compared to controls. Antibiotics are recognized to play a key role in managing septic complications of IBD in humans, however, their role in the intentional modulation of the intestinal microbiota to prevent or treat active inflammation is not well studied and is controversial. Results from animal studies highlight the complex nature of the interaction of the intestinal microbiota and the host. Some studies have shown that antibiotics can prevent and/or ameliorate colitis in IL-10-/- mice and certain antibiotic regimens can actually worsen colitis in DSS-treated mice. The microbiota of the gastrointestinal tract is a highly complex and understudied population of microbes. Because a majority of the organisms in the gut cannot be cultivated non -culture based techniques using the conserved 16S rDNA sequence (T-RFLP and clone library analysis) are being used to enable a more detailed examination of the intestinal microbiota. 16S rDNA data can be used to compare diversity, which is measured by the richness (total number of species) and evenness (relative abundance of each species) within and between microbial communities. The availability of on-line analysis tools allows one to use ecological measures to investigate changes in diversity of a microbial community influenced by such things as antibiotic use. T-

RFLP and clone library analysis were used to compare the effects of antibiotic treatment to untreated controls on the mucosa-associated microbiota of C57BL/6 IL-10-/- mice. Groups of animals were either treated with streptomycin or a combination of amoxicillin, metronidazole, and bismuth. T-RFLP and clone library analysis revealed that both antibiotic regimens resulted in marked, reproducible shifts in the community structure of the mucosal microbiota.

Introduction

Crohn's patients have a Th1 exaggerated immune response to their own intestinal microbiota and IBD develops in the areas of highest bacterial concentration, thus incriminating the microbiota in the initiation of disease (30). Additionally, diversion of the fecal stream is associated with distal improvements in IBD patients (30). Studies show there are differences in the mucosa-associated bacteria in IBD patients compared to controls. A reduction in diversity with loss of beneficial organisms such as *Lactobacillus* and *Bifidobacterium* and an increase in mucosa-associated bacteria and invasion occur in IBD patients (57, 72, 79, 85, 90). These lines of evidence have led to the proposal that using antibiotics or probiotics to alter the microbiota may be therapeutic in IBD.

Antibiotics are recognized to play a key role in managing septic complications of IBD in humans, however, their role in the intentional modulation of the intestinal microbiota to prevent or treat active inflammation is not well studied and is controversial (98). Results from animal studies have shown that antibiotics can prevent and/or ameliorate experimental colitis in IL-10-/- mice (67). It has been found that antibiotics with different microbicidal activity had differential effectiveness thereby suggesting different subsets of the intestinal microbiota were responsible for the induction and or maintenance of colitis (47). Certain antibiotic regimens can actually increase the severity of IBD in DSS-treated mice thus emphasizing the importance of the specific nature of antibiotic-associated alteration in the intestinal microbiota (92). This highlights the complex

nature of the interaction between the host and the indigenous microbiota. The microbiota of the gastrointestinal tract is a highly complex and understudied population of microbes of over 400 different species.

Because a majority of the organisms in the gut cannot be cultivated non - culture based techniques using the conserved 16S rDNA sequence (T-RFLP and clone library analysis) are being used to enable a more detailed examination of the intestinal microbiota. These non-culture based techniques have been traditionally used to study environmental microbial ecology. However, it is becoming increasingly common to utilize these methods to study the microbial communities of humans.

16S rDNA data can be used to compare overall diversity, which is measured by the richness (total number of species) and evenness (relative abundance of each species) within and between microbial communities. The Ribosomal Database Project - II (RDP-II) in the Center of Microbial Ecology at Michigan State University (MSU) contains over 250,000 16S rRNA sequences along with many useful online analysis tools (http://rdp.cme.msu.edu). Computer programs are available such as Distance-Based OTU and Richness (DOTUR) and EstimateS (http://viceroy.eeb.uconn.edu/EstimateS) enabling one to easily compute standard ecological measures of diversity (99). To compare the richness and evenness of several libraries at once the program f-LIBSHUFF is very useful (38). T-RFLP profiles from several different samples can be statistically compared to one another by using analytical tools from the Initiative

for Bioinformatics and Evolutionary Studies (I-BEST) website

(http://www.ibest.uidaho.edu/tools/trflp_stats) (1). The availability of these on-line analysis tools allows one to use ecological measures to investigate changes in diversity of a microbial community influenced by such things as antibiotic use.

With our established specific pathogen free C57BL/6 mouse colony we have a well-defined controlled environment to conduct studies to determine the effects of antibiotic use on the overall community structure of the mucosa-associated microbiota. Non-culture based techniques, T-RFLP and clone library analysis were used to compare the effects of antibiotic treatment to untreated controls on the mucosa-associated microbiota of IL-10-/- mice.

Materials and Methods

Animals and housing.

A colony of C57BL/6 IL-10 -/- mice were housed and maintained in a specific pathogen free environment at Michigan State University (MSU). Sixteen week old female animals were randomly selected from our breeding colony and placed into three cages containing 5 animals each. These animals were transferred to the animal containment facility for antibiotic treatment. The MSU All University Committee on Animal Use and Care approved all animal protocols were used. Food, water and bedding were autoclaved before use. The mice were kept on a 12 – hour light/dark cycle.

Antibiotic treatment.

The fifteen C57BL/6 IL-10 -/- mice were divided into three treatment groups including: untreated, Streptomycin treated, and a triple antibiotic treatment of amoxicillin, metronidazole, and bismuth. Streptomycin was administered in their drinking water 5g/L. The triple antibiotic treatment was administered via food pellets by BioServ with the following concentration per pellet (3 mg/tablet of amoxicillin) (0.69 mg/tablet of Metronidazole) and (0.185 mg/tablet of bismuth) (Frenchtown, NJ). The duration of treatment was 7 days.

Sample collection.

The mice were sacrificed via CO₂ asphyxiation and gastrointestinal necropsy was performed. The cecum was removed by transection of the terminal ileum and the proximal colon. The cecal apex was removed by transection midway down its length at the sharpest point of the curve. The apex was washed thoroughly in 1 X phosphate buffered saline and sectioned longitudinally into three pieces that were snap frozen in a dry ice/ethanol mixture and stored at -80 °C.

DNA extraction.

DNA was extracted from one cecal apex section from each animal using the Qiagen DNeasy tissue kit (Germantown, MD). The manufacture's instructions were followed with the exception of the 55°C incubation was extended to overnight and the secondary lysis step was extended to 30 min at 70°C.

Terminal Restriction Length Polymorphism (T-RFLP).

T-RFLP was performed on all DNA samples as previously described (58). The 16S gene was amplified by PCR using the bacterial primers 8F/6-FAM labeled (Integrated DNA technologies, Coralville, IA) and 1492R unlabeled (101) (Table 2). The PCR products were purified using GFX[™] (Amersham Phamacia Biotech). The purified PCR products were cut using the restriction enzyme Msp I (New England Biolabs, Beverly, MA). Samples were subjected to capillary

electrophoresis using an ABI Prism® 3100 (Applied Biosystems Instruments, Foster City, CA) in Genescan mode. The 6-FAM labeled 8F primer enabled the terminal restriction fragments (T-RFs) to be visualized. GeneScan 3.7 was used to calculate the sizes and abundances of the fragments.

Analysis of T-RFLP profiles.

Analysis of T-RFLP was performed in a manner to allow comparison of profiles using standard measures of ecologic diversity. A computer program that uses a statistical method for analysis of multiple T-RFLP profiles was used to group (bin) (1). Once the TRFs were binned a similarity matrix was produced that indicated the relative proportion of each group for each sample. The Bray-Curtis similarity index was calculated as: $C_N = \frac{2jN}{N_a + N_b}$, where N_a is the total number

of T-RFs in sample A and N_b is the total number of T-RFs in sample B, and 2jN is the sum of the lower of the 2 abundances for the T-RFs found in both samples. This calculation was performed for each pair-wise comparison was calculated by importing the similarity matrix into the program EstimateS (http://viceroy.eeb.uconn.edu/EstimateS). To provide a visual method for the comparison of multiple samples, unweighted pair group method with arithmetic mean (UPGMA) trees were constructed using MEGA3 (60).

Clone libraries.

The 16S gene was amplified by PCR using unlabeled bacterial primers 8F and 1492R (101). The PCR reaction was carried out as stated above in the T-RFLP procedure with the exception of the use of 20 cycles instead of 30 cycles and a 52 °C annealing temperature. The PCR products were purified using GFX™ purification (Amersham Phamacia Biotech). The resulting PCR product was ligated into the pCR 2.1 TOPO cloning vector (Invitrogen, Carlsbad, CA). Ninety – six white colonies were selected from each library and grown in 96 deep well plates containing LB freezing broth containing 4% v/v glycerol and carbenicillin (50µg/ml) overnight at 37°C. A screening PCR was performed using M13 forward and reverse primers (Table 2). PCR of the cloned product was carried out using Invitrogen reagents (Invitrogen, Carlsbad, CA). Each 25µl reaction contained (1.5µl of the *E. coli* overnight growth, 80µM of a dNTP mixture, 100 fmol of each M13 primer, 1U of Tag DNA polymerase in a final concentration of 20 mM Tris-HCl, 50 mM KCl, and 1mM MgCl₂). Initial denaturation of DNA template was carried out at 95°C for 5 minutes this was followed by 30 cycles of 95°C for 30 seconds, 55°C for 1 minute, 72°C for 3 minutes; with a final extension of 70°C for 10 minutes. The PCR amplicons were quality checked using E-GEL® 96 (Invitrogen, Carlsbad, CA). The amplicons of the correct size of approximately 1500 bps were processed by ExoSAP-IT (USB Corporation, Cleveland, OH). Each ExoSAP-IT reaction contained (0.25 μ l

ExoSAP-IT, 3.25 μ I sterile water, and 1.5 μ I of M13 PCR product). The reactions were incubated for 30 minutes at 37 °C followed by 80 °C for 15 minutes. The processed M13 PCR products were submitted to the Research Technology Support Facility (RTSF) at Michigan State University for sequencing using either the 531R or 8F primers (Table 2).

The raw sequence data were processed through an automated "information pipeline" Ribosomal Database Project (RDP) (rdp.cme.msu.edu). Through this pipeline the sequences were quality scored, trimmed, and the vector sequence was removed. The resulting trimmed sequences were subjected to secondary alignment and a RNA distance matrix was produced. This RNA distance matrix was imported into DOTUR and EstimateS to calculate standard ecological diversity measurements Shannon-Weiner and Chao1, to compare overall diversity (richness and evenness) within and between communities (99).

The Shannon-Weiner diversity index was calculated as: $H = -\sum_{i=1}^{i=S} p_i \ln p_i$ where p_i

is the proportion of the ith sequence relative to the sum of all sequences. The

Chao1 index of richness was calculated as: $S_{chao1} = S_{obs} + \frac{F_1^2}{2F_2}$, where S_{obs} is

the number of molecular species in the sample, F₁ is the number of observed molecular species represented by singletons, and F2 is the number of observed molecular species represented by doubletons. Coverage estimations were calculated by the method of Good (43) using the calculation of [1-(n/N)]x100,

where n= number of molecular species represented by one clone and N is the total number of sequences in the library. Statistical differences in the compositions of clone libraries from the untreated and antibiotic treated samples were determined using f-LIBSHUFF (http://www.plantpath.wisc.edu/joh/s-libshuff.html) (100). The percent proportion of the sequences classified into phyla by the Ribosomal Database Project Library Compare (Libcompare) for each of the clone libraries from the antibiotic treated and untreated animals (http://rdp.cme.msu.edu).

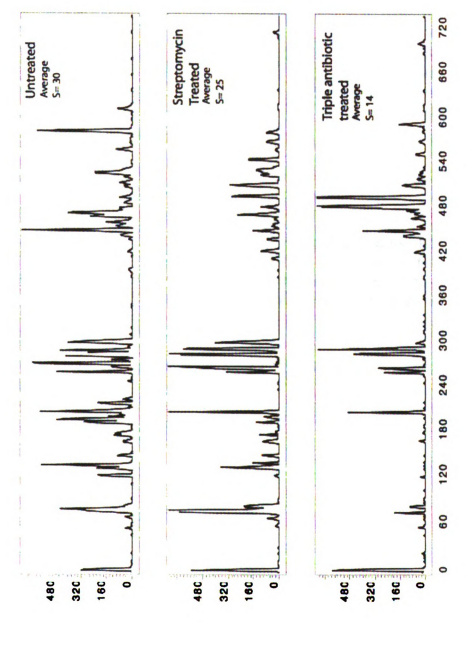
Results

T-RFLP analysis.

Fifteen C57BL/6 IL-10-/- mice were divided into untreated, streptomycin treated and triple antibiotic treated groups, 5 mice each. Seven days following antibiotic administration gastrointestinal necropsy was performed in which the cecal tip was taken and cleared of luminal contents. The cecal tissue was transected longitudinally into three sections and snap frozen for DNA extraction. None of the animals represented with clinical signs of sickness or gross pathology at necropsy.

DNA extraction was performed on frozen tissue and analyzed via T-RFLP using restriction enzyme *Mspl*. Visual inspection of the T-RFLP traces revealed there was a reduction in the number of T-RFs seen (richness) with antibiotic treatment compared to no treatment (Figure 13). Within the treatment groups the traces for each of the 5 animals were very similar (data not shown). To

associated community structures of the untreated and antibiotic treated animals analysis was performed using analytical tools from the IBEST website (http://www.ibest.uidaho.edu/tools/trflp_stats) (1). A UPGMA dendrogram was produced using a matrix with the distance measurements (1- Bray-Curtis) (Figure 14). Each treatment group distinctly grouped together demonstrating the communities within the treatment groups are more similar to one another than between treatment groups.



visual inspection distinct differences can be detected between the three treatement groups. For each trace the number of Figure 13. Representative T-RFLP traces for untreated, streptomycin treated, and triple antibiotic treated animals. Upon peaks (S) is shown.

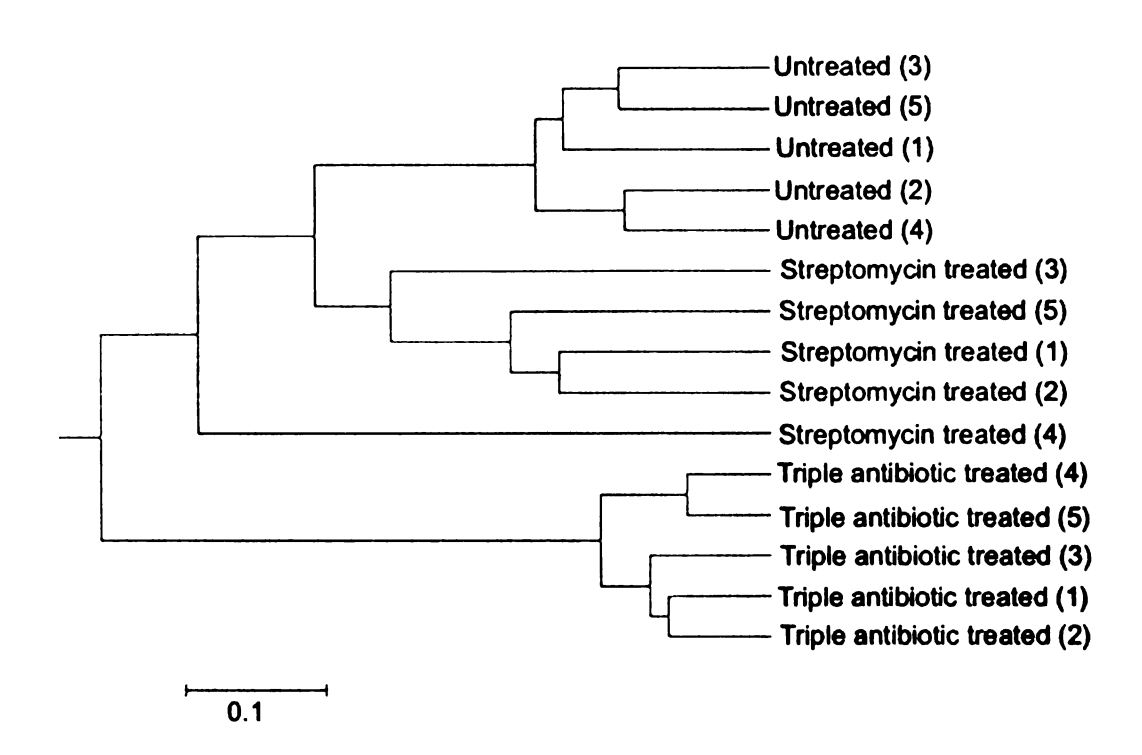


Figure 14. UPGMA dendrogram created using Bray-Curtis distances (1-Bray-Curtis) calculated from T-RFLP analysis of IL-10-/- mice treated with antibiotics compared to untreated controls. Reproducible changes in the community structure of the mucosa-associated microbiota were detected when comparing the streptomycin and triple antibiotic treated groups to the untreated group of animals.

Clone library analysis.

Clone library analysis was also performed to examine the cecal mucosaassociated microbial communities of the antibiotic treated compared to untreated animals. DNA from the cecal tissue of antibiotic treated and untreated animals was used to amplify the 16S rRNA genes using the same bacterial primers used for T-RFLP analysis. The resultant amplicons were cloned into a T-tailed plasmid vector, and the DNA sequence was determined for a set of randomly selected clones from each library. These sequences were processed through an automated "information pipeline" Ribosomal Database Project (RDP) (rdp.cme.msu.edu). UPGMA trees were constructed using the distance measurement (1-Bray-Curtis) (Figure 15). Again, similar grouping is seen as with the T-RFLP profiles. This not only supports the reproducible changes observed in overall diversity caused by antibiotic treatment but it also demonstrates the utility of the T-RFLP analysis that is a less expensive high-throughput method to examine microbial communities. However, clone library analysis enables one to obtain more information of the microbial community such as identification of the organisms adversely affected by the

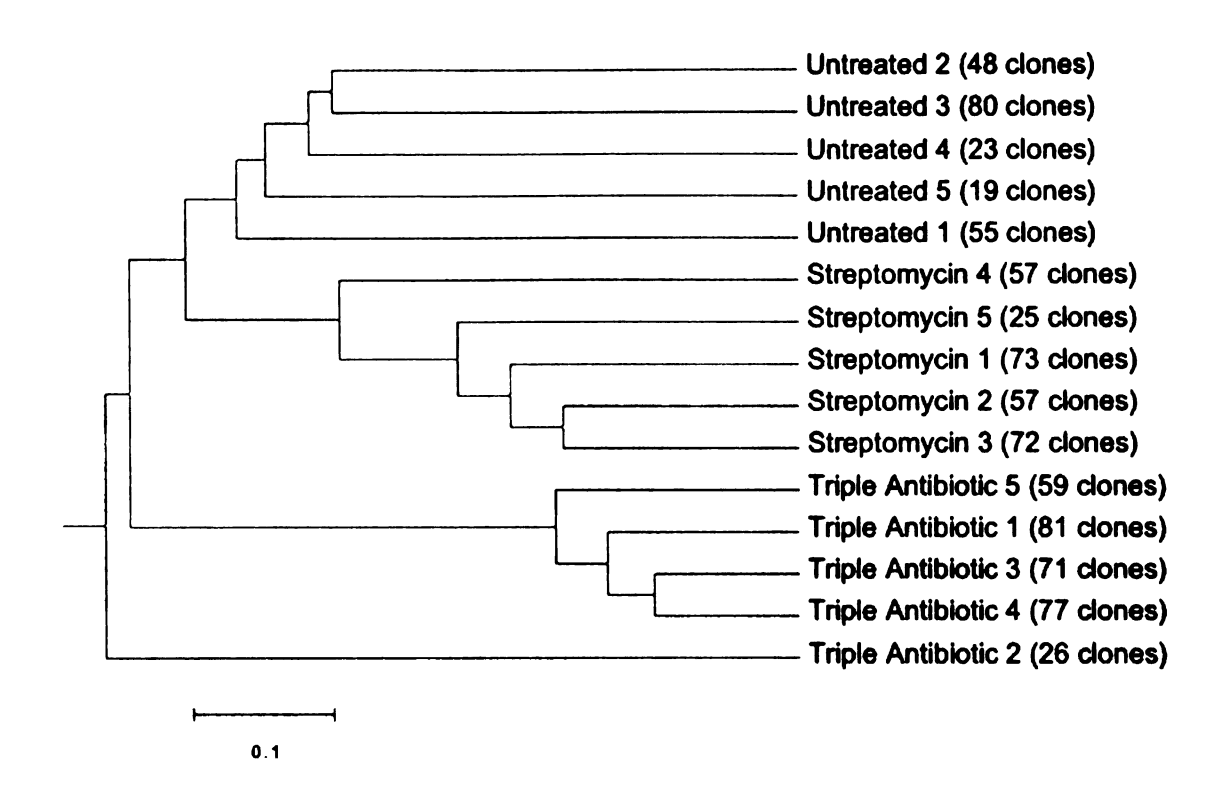
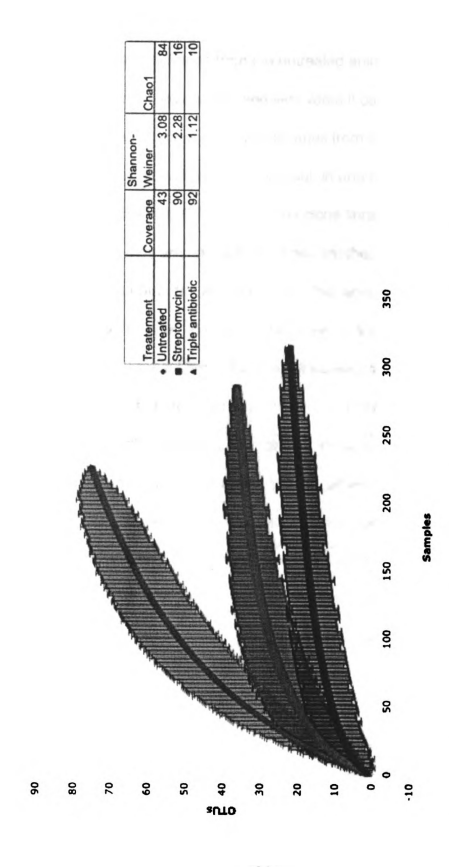


Figure 15. UPGMA dendrogram created using Bray-Curtis distances (1-Bray-Curtis) calculated from clone library analysis of IL-10-/- mice treated with antibiotics compared to untreated controls. The number of clone having sequences greater than 350 base pairs is listed next to each library. Reproducible changes in the community structure of the mucosa-associated microbiota were detected when comparing the streptomycin and triple antibiotic treated groups to the untreated group of animals.

The sequences from each treatment group were pooled to construct rarefaction curves (Figure 16). There was a dramatic decrease in the number of OTUs observed (grouped as 97% similarity) when comparing the untreated animals to the Streptomycin and triple antibiotic treated animals with the average of 78, 14, and 8 OTUs respectively. The Shannon-Weiner index was used to calculate the overall diversity and the Chao1 index was used to calculate the estimated richness for each sample and the values for the samples within the treatment groups were averaged (Figure 16). The average Shannon-Weiner index and the Chao1 index decreased with antibiotic treatment. There was a more dramatic decrease with the triple antibiotic treatment as compared to the Streptomycin treatment. Together, these data demonstrate a drastic reduction in overall richness and evenness caused by antibiotic treatment.



represented by sample number on the X-axis. On the Y-axis is the operational taxonomic units (OTUs) defined by 97% compared to antibiotic treated animals. The clone libraries from five animals in each treatment group were combined, Figure 16. Rarefaction curves representing the richness of the mucosa-associated microbiota in untreated animals sequence similarity.

Statistical differences in the compositions of the clone libraries from the three treatment groups was determined using \(\int \text{LIBSHUFF} \) (100) (Table 6). When comparing the clone libraries from the untreated animals to the clone libraries of the streptomycin treated animals and vice versa it can be seen that the results are not very clear. In some cases the libraries from the untreated animals were subsets on one another and vice versa. But, in one case a library from an untreated animal is very different than the clone libraries from the streptomycin treated animals, they are not subsets of one another. When comparing the clone libraries from the untreated animals to the triple antibiotic treated animals and vice versa it can be seen that two of the clone libraries from the triple antibiotic treated animals are a subset of the clone libraries from the untreated animals and the clone libraries from the untreated animals are very different from the libraries from the triple antibiotic treated animals. When comparing the clone libraries from the streptomycin treated animals to the clone libraries from the triple antibiotic treated animals and vice versa it is clear that the clone libraries are very different from one another, they are not subsets of each other.

Library Compare through the RDP website (http://rdp.cme.msu.edu) was used to classify the aligned sequences from each library into phyla. The percent proportion of sequences categorized into each represented phylum was calculated for each library (Table 7). There is an increased proportion of *Bacteriodetes* and a decreased proportion of *Firmicutes* in the libraries from the streptomycin treated animals as compared to the libraries from the untreated

animals. There is a dramatic increase in the phylum *Proteobacteria* and a decrease in the phyla *Bacteriodetes* and *Firmicutes* in the libraries from the triple antibiotic treated animals as compared to the libraries from the untreated animals.

	2	0	0	0	0.0005	0.0063	0	0	0	0	0	0,8063	0,3906	0.5671	0.0358	0
	4	0	0	0	0	0	0	0	0	0	0	0,1626	0.1577	0.3189	0	0.0013
TA	3	0	0	0	0.003	0.0035	0	0	0	0	0	0.8861	0.1527	0	0.054	0.7908
	2	0	0	0	0	0	0	0	0	0	0	0.0136	0	0.0464	0.0034	0.0013
	-	0	0	0	0	0	0	0	0	0	0	0	0.2164	0.5256	0.0729	0.0425
	2	0	0.0002	0	0	0.0003	0.0012	60000'0	0	0.0011	0	0	0	0	0	0
S	4	0	0	0	0.1239	0.6014	0.0025	0.1482	0	0	0.1864	0	0	0	0	0
	3	0	0.0038	0	0.9636	0.567	0.0275	0.2206	0	0.0007	0.016	0	0	0	0	0
	2	0	0.0002	0	0.061	0.6243	0.0791	0	0.1744	0.0174	0	0	0	0	0	0
	-	0	0	0	0.5665	0.7465	0	0.2721	0.0009	0.0007	0.9014	0	0	0	0	0
	2	0.0785	0.7927	0.6626	0.7349	0	0	0	0	0.0001	0	0	0	0	0	0
D	4	0.5249	0.8255	0.9145	0	0.6926	0.0118	0.0014	0.0113	0.0015	0.0007	0	0	0	0	0
	3	0.0684	0.0982	0	0.5843	0.6688	0.0002	0.026	0.0004	0.0002	0.7485	0	0	0	0	0
	2	0.001	0	0.2977	0.8593	0.3826	0.0042	0.0526	0.0115	0.0004	0.0271	0	0	0	0	0
	-	0	90000	0.012	0.789	0.272	0	0	3	0	0	0	0	0	0	0
/	/ ×	-	N	۳ ص	4	2	-	2	n	4	5	-	TA 2	3	4	5

streptomycin treated (S), and the triple antibiotic treated (TA) animals. P values are shown for all coverage comparisons. Table 6. S-LIBSHUFF was used to make all pair-wse comparison between the 15 clone libraries from the untreated (U), Multiple comparisons were made therefore the Bonferonni correction was performed along with the calculation of the Monte Carlo error. The generated a minimum P value= 0.0002.

Average	0.0	15.6	84.4		0.0	63.4	37.5		71.8	3.4	24.8
5	0.0	27.8	72.2	5	0.0	54.5	50.0	5	57.6	8.5	33.9
4	0.0	9.1	90.9	4	0.0	63.6	36.4	4	66.2	2.8	31.0
3	0.0	11.7	88.3	က	0.0	57.4	42.6	3	70.0	4.3	25.7
2	0.0	23.8	76.2	2	0.0	82.1	17.9	2	88.5	0.0	11.5
1	0.0	5.6	94.4	1	0.0	59.2	40.8	1	76.6	1.3	22.1
Untreated	Proteobacteria (-)	Bacteriodetes (-)	Firmicutes (+)	Streptomycin treated	Proteobacteria (-)	Bacteriodetes (-)	Firmicutes (+)	Triple antibiotic treated	Proteobacteria (-)	Bacteriodetes (-)	Firmicutes (+)

Table 7. The percent proportion of the sequences classified into phyla by the Ribosomal Database Project Libcompare for each of the 15 clone libraries. Major differences are detected when comparing the classification of the sequences into the proportion of Proteobacteria along with a decrease in both Bacteriodetes and Firmicutes are observed in the libraries from three different phyla. An increased proportion of Bacteriodetes and a decreased proportion of Firmicutes are observed in he libraries from the streptomycin treated animals as compared to the untreated controls. A major increase in the the triple antibiotic animals as compared to the untreated controls.

Discussion

Clinical and experimental studies have implicated the microbiota in the perpetuation of inflammatory bowel disease. However, it is not know what groups of bacteria are primarily responsible. The use of antibiotic and probiotic (live microorganisms that confer benefit to the host when consumed) regimens exert beneficial effects in humans and animal models (42, 66, 67, 74, 88). The effects of antibiotics and/or probiotics on the intestinal microbial community is not well studied.

In this study we utilized a total of 15 C57BL/6 IL-10-/- mice raised in a specific pathogen free environment to study the effects of antibiotic treatment (either streptomycin or a combination of amoxicillin, metronidazole, and bismuth) on the microbial community of the intestinal mucosa. With both methods of T-RFLP and clone library analysis a drastic reproducible decrease in the overall diversity of the intestinal microbiota was observed in the antibiotic treated mice as compared to the untreated mice.

By visually inspecting the T-RFLP traces a decrease in richness (number of T-RFs) was observed when comparing the antibiotic treated animals to the untreated animals. Visual inspection of the T-RFLP traces determined reproducibility of this method because the traces were more similar to one another within treatment groups then between treatment groups. This was further supported by the statistical analysis of the traces and the use of the Bray-Curtis similarity index which compares the microbial communities to one another taking

into account the richness (number of T-RFs) and evenness (abundance of each T-RF) of the microbial communities.

The Bray-Curtis dendrogram created from the clone library data showed the animals from the three treatment groups again distinctly grouped together within their own treatment group. This supports the T-RFLP data. The sequences from each of the treatment groups were pooled to construct rarefaction curves. Rarefaction curves are used to visually represent the overall richness and to evaluate the sampling intensity of the microbial communities. It can be seen by the rarefaction curves that the richness (represented by the number of OTUs) of the microbial communities from the antibiotic treated animals is much lower than that of the untreated animals. This was further supported by the average values obtained from the Chao1 estimator of richness for each of the three treatment groups. The Chao1 richness estimate for the untreated animals was much greater than the estimates for the antibiotic treated animals. It can also be seen by the shape of the rarefaction curves that the sampling intensity of the microbial communities from the untreated animals is not as great as the microbial communities from the antibiotic treated animals. This was also demonstrated by the average coverage calculations. The average coverage for the Streptomycin and the triple antibiotic groups was 90 and 92% whereas the average coverage of the microbial communities from the untreated animals was only 43%. Coverage was not equal between the three treatment groups. To remedy this

problem more sampling will need to be accomplished for the microbial communities of the untreated animals and this will allow for better comparisons.

Statistical differences in the compositions of the clone libraries from the three treatment groups was determined using \(\int \text{LIBSHUFF} \) (100). A small P value for $\Delta C(xy)$ coupled with a high P value for $\Delta C(yx)$ indicates sequences in Y are a sub-sample of sequences in X (103). When comparing the clone libraries from the untreated animals to the clone libraries of the streptomycin treated animals and vice versa it can be seen that the results are not very clear. In some cases the libraries from the untreated animals were subsets on one another and vice versa. But, in one case a library from an untreated animal is very different than the clone libraries from the streptomycin treated animals, they are not subsets of one another. When comparing the clone libraries from the untreated animals to the triple antibiotic treated animals and vice versa it can be seen that two of the clone libraries from the triple antibiotic treated animals are a subset of the clone libraries from the untreated animals and the clone libraries from the untreated animals are very different from the libraries from the triple antibiotic treated animals. Finally, when comparing the clone libraries from the streptomycin treated animals to the clone libraries from the triple antibiotic treated animals and vice versa it is clear that the clone libraries are very different from one another, they are not subsets of each other. This makes sense based on the mode of action for the different antibiotics used. These \(-LIBSHUFF \) results may be confusing because the amount of coverage is not even amongst the three

treatment groups. Therefore, the comparisons made between the streptomycin and triple antibiotic treated groups are more solid because of similar coverage values. The Shannon-Weiner index, a measurement of the overall diversity within a community, was also used to compare the three treatment groups to one another. There was a decrease in overall diversity when comparing the untreated to the streptomycin and triple antibiotic treated animals with the average Shannon-Weiner values of 3.08, 2,28, and 1.12.

The sequences for each of the samples were classified into phyla by using a comparison tool from the Ribosomal Database Project website (http://rdp.cme.msu.edu). All of the sequences from the untreated mice fell into the phyla Bacteriodetes or Firmicutes. Bacteriodetes is composed of three large classes of bacteria: the Bacteriodes, Flavobacteria, and the Sphingobacteria (24). Of the three groups the only the class Bacteriodes was found in the intestinal microbial community of the untreated mice. This is expected considering Bacteriodes are found primarily as a commensal intestinal organisms (7, 125). Bacteriodes are anaerobic, gram-negative, rod shaped bacteria (24). The phylum Firmicutes is divided into the classes Clostridia, Bacilli, and the Mollicutes (24). A majority of the intestinal microbes of the untreated mice were in the class Clostridia. Clostridia are obligate anaerobes, gram-positive, cocci shaped bacteria (24).

There was an increased proportion of *Bacteriodetes* and a decreased proportion of *Firmicutes* in the libraries from the streptomycin treated animals as

compared to the libraries from the untreated animals. Streptomycin is an aminoglycoside that damages cell membranes and inhibits protein synthesis. It is particularly effective against aerobic gram-negative bacteria. There was an increase in the number of anaerobic gram negatives and a decreased number of anaerobic gram-positive organisms as represented by the *Bacteriodetes* and *Firmicutes* phyla respectively.

There is a dramatic reproducible shift in the microbial communities of the triple antibiotic treated animals as demonstrated by a large increase in the phylum Proteobacteria and a decrease in the phyla Bacteriodetes and Firmicutes as compared to the libraries from the untreated animals. The phylum Proteobacteria is divided into five sections referred to as alpha, beta, gamma, delta, and epsilon (24). The dramatic increase in *Proteobacteria* was due to the dramatic increase in the order Enterobacteriales which falls in the class gammaproteobacteria. Enterobacteriales are facultative anaerobes, gramnegative, rod shaped bacteria (24). Amoxicillin is a moderate spectrum betalactam which inhibits cross-linkage between linear peptidoglycan polymer that makes up the major component of cell walls of gram positives. This explains the dramatic decrease in the *Firmicutes*. Metronidazole is selectively taken up by anaerobic bacteria and inhibits nucleic acid synthesis. This antibiotic would target both Bacteriodetes and Firmicutes considering bacteria in both of these phyla are anaerobic. Therefore, the decrease in these two major phyla of bacteria enabled members of the phyla *Proteobacteria*, an otherwise minor component of the

microbiota, (undetectable in the untreated animals), to become dominant. Alterations in the intestinal microbiota such as these can be detrimental to the host. An overgrowth of *Clostridium difficile*, a toxigenic bacterium, can occur in the intestinal microbiota due to antibiotic use (80). This can lead to antibiotic associated pseudomembraneous colitis (80). Non - Clostridium difficile antibiotic associated diarrhea is another example of a condition that can occur due to major shifts in the intestinal microbiota brought on by antibiotic use (123). Non-C. difficile antibiotic associated diarrhea is caused by the decrease in metabolically beneficial bacteria primarily responsible for breaking down otherwise indigestible carbohydrates to short chain fatty acids. Due to this increase in indigestible carbohydrates there is an increase in the osmotic load in the intestines resulting in diarrhea (123). This demonstrates that although it may be tempting to administer antibiotics long term for Crohn's disease patients it would be more beneficial to first understand the changes in the intestinal microbial community caused by different antibiotics. Additionally, a greater understanding of the intestinal microbial community and the identification of the main groups of bacteria responsible for the perpetuation of inflammatory bowel disease would lead to better treatment options.

In this study we utilized the non-culture based techniques of T-RFLP and clone library analysis, to examine the changes that occur in the intestinal microbial community structure with antibiotic administration. A dramatic decrease in the overall diversity of the intestinal microbial community of the antibiotic

treated animals was observed as compared to the untreated animals. Importantly these effects were reproducible from animal to animal in each treatment group.

Chapter 5

Summary and Synthesis

It is undisputed that the microbiota plays a definite role in the development and/or maintenance of the inflammation observed in inflammatory bowel disease. There are several lines of evidence from human and animal studies including: an abnormal immune response to their own microbiota, differences in the mucosaassociated microbiota of diseased versus non-diseased tissue, and the effectiveness of some antibiotic and probiotic regimens (30, 57, 72, 85, 88). Perhaps the most convincing is that when the antigenic source (the microbiota) is removed either by diversion of fecal stream in human studies or by use of germfree animal models, colitis is ameliorated (30). The intestinal microbiota serves many important functions in the gut that mammals are not able to perform on their own, such as vitamin synthesis, digestion of complex carbohydrates into short-chain fatty acids, and colonization resistance. Therefore, it is not appropriate to just rid the IBD patients of the microbiota entirely by antibiotic use. A balance has to be obtained. If we can determine the main culprits in the substantiation of inflammation in the intestinal microbiota then better treatment methods can be utilized such as antibiotic, probiotic, and prebiotics. Even though the microbiota plays a significant role in the inflammation observed in IBD and serves very important functions it is still a vastly understudied microbial community. Unfortunately, human studies of the intestinal microbiota are complicated by the fact that a large amount of variation is observed between individual's microbiota. This variation may be due to differences in environment, diet, genetic background, and disease state. Fortunately the use of animal

models and non-culture based techniques can be used to study the microbiota in a controlled environment. Currently, there are several on-line analytical tools that are being used to study the impact of different factors on the overall diversity (richness of evenness) of a microbial community (1, 99, 100). These tools are being utilized to study the changes in diversity within a community (alpha diversity) and between microbial communities (beta diversity).

In the studies presented, non-culture based methods were used to examine the structure and dynamics of the mucosa-associated microbiota under various ecologic stresses of pathogen invasion, host genotype, and antibiotic usage. Two methods to examine the microbiota using retrieval of 16S rRNA gene sequence data were used; terminal restriction fragment length polymorphism (T-RFLP) analysis and 16S clone library construction. Both of these methods provide insight into the species richness and evenness of a given community. This also allows comparisons to be made between communities with the eventual goal of relating ecosystem structure with function.

We used examination of microbial ecology to determine the effect of colonization of the cecal mucosa by wild-type strain and a mutant strain (CDT deficient) of *H. hepaticus* (58). We used both T-RFLP analysis and clone library analysis to examine how stable colonization of the mucosal by *H. hepaticus* affected the overall community structure. Wild-type *H. hepaticus* rapidly became a dominant member of the microbiota and decreased the overall diversity of the community (58). The CDT deficient strain of *H. hepaticus* showed delayed

kinetics however, eventually reached similar levels of colonization. These results suggest that CDT production by *H. hepaticus* represents a bacterial adaptation that allows long-term persistence within the mammalian host (89). When comparing the IL-10-/- and IL-10+/+ animals infected with either wild-type (CDT+) or mutant (CDT-) H. hepaticus to the uninfected controls, Inflammation appeared to have an effect on the composition of the microbiota. There have been studies investigating the effect of inflammation on the microbiota in human and animals studies of non-diseased versus diseased tissue within and between individuals. These studies have concluded mixed results (9, 10, 48). A question still remains whether a difference observed in the composition of the microbiota between the non-IBD and IBD patients has to do with a cause or effect of the diseased state. With our Crohn's disease mouse model, C57BL/6 IL-10-/- mouse infected with H. hepaticus, disease is only present when the microbiota along with wild-type (CDT+) H. hepaticus is present. Disease is much less severe when a C57BL/6 IL-10-/- mouse is infected with a mutant (CDT-) H. hepaticus, thus allowing for the investigation of whether or not inflammation had an affect on the microbial community (121). Studying the cecal mucosa-associated microbiota of our Crohn's disease mouse model in controlled environment demonstrates that inflammation does effect the composition of the microbiota. Additionally, host genotype had an effect on the composition of the microbiota. These changes were reproducible from animal to animal as the overall community structure of infected animals was shifted away from that seen in uninfected animals.

The effect of host genotype on the establishment of the indigenous microbiota was examined further by comparing sibling IL-10-/- and wild type animals generated by mating of heterozygous parents. At the time of weaning (4 weeks of age), the microbial communities could be grouped by the genotype of the mouse. With increasing age, these differences were less apparent, perhaps reflecting a greater influence of diet or the loss of the effect of breast milk on the on community composition.

Finally, since antibiotics have been used to prevent or ameliorate inflammatory bowel disease in animals models and in selected human cases, we wished to determine what effect antibiotic administration would have on the mucosal microbiota. Groups of animals were treated with either streptomycin or the combination of amoxicillin, metronidazole and bismuth. T-RFLP and clone library analysis revealed that both antibiotic regimens resulted in marked, reproducible shifts in the community structure of the mucosal microbiota. The antibiotics severely diminished the overall diversity, mostly due to a drastic reduction in overall species richness.

Taken together our results indicate that the community structure of the indigenous mucosal microbiota can be determined and followed by the use of the non culture-based techniques used throughout this thesis. More importantly, comparison between multiple animals suggests that ecologic stressors (e.g. alterations in host genotype, antibiotic administration and invasion by a pathogen) can result in drastic and reproducible alteration in the community

structure. If we were to develop a greater understanding of the factors that shape and maintain the structure of the indigenous microbiota of the gut, this should result in novel treatment modalities for IBD based on rationale manipulation of the intestinal microbiota.

References

- 1. Abdo, Z., U. M. Schuette, S. J. Bent, C. J. Williams, L. J. Forney, and P. Joyce. 2006. Statistical methods for characterizing diversity of microbial communities by analysis of terminal restriction fragment length polymorphisms of 16S rRNA genes. Environ Microbiol 8:929-38.
- 2. **Abreu, M. T.** 2005. Nod2 in normal and abnormal intestinal immune function. Gastroenterology **129:**1302-4.
- 3. Abreu, M. T., M. Fukata, and M. Arditi. 2005. TLR signaling in the gut in health and disease. J Immunol 174:4453-60.
- 4. Asahara, T., K. Shimizu, K. Nomoto, T. Hamabata, A. Ozawa, and Y. Takeda. 2004. Probiotic bifidobacteria protect mice from lethal infection with Shiga toxin-producing *Escherichia coli* O157:H7. Infect Immun 72:2240-7.
- 5. Avaniss-Aghajani, E., K. Jones, D. Chapman, and C. Brunk. 1994. A molecular technique for identification of bacteria using small subunit ribosomal RNA sequences. Biotechniques 17:144-6, 148-9.
- Avaniss-Aghajani, E., K. Jones, A. Holtzman, T. Aronson, N. Glover,
 M. Boian, S. Froman, and C. F. Brunk. 1996. Molecular technique for rapid identification of mycobacteria. J Clin Microbiol 34:98-102.
- 7. Backhed, F., R. E. Ley, J. L. Sonnenburg, D. A. Peterson, and J. I. Gordon. 2005. Host-bacterial mutualism in the human intestine. Science 307:1915-20.
- 8. **Bamias, G., M. R. Nyce, S. A. De La Rue, and F. Cominelli.** 2005. New concepts in the pathophysiology of inflammatory bowel disease. Ann Intern Med **143:**895-904.
- 9. **Bibiloni, R., M. Mangold, K. L. Madsen, R. N. Fedorak, and G. W. Tannock.** 2006. The bacteriology of biopsies differs between newly diagnosed, untreated, Crohn's disease and ulcerative colitis patients. J Med Microbiol **55:**1141-9.
- 10. **Biblioni, R., M. A. Simon, C. Albright, B. Sartor, and G. W. Tannock.** 2005. Analysis of the large bowel microbiota of colitic mice using PCR/DGGE. Lett Appl Microbiol **41:45-51**.

- 11. Blackwood, C. B., T. Marsh, S. H. Kim, and E. A. Paul. 2003. Terminal restriction fragment length polymorphism data analysis for quantitative comparison of microbial communities. Appl Environ Microbiol 69:926-32.
- 12. **Bohnhoff, M., B. L. Drake, and C. P. Miller.** 1954. Effect of streptomycin on susceptibility of intestinal tract to experimental Salmonella infection. Proc Soc Exp Biol Med **86:**132-7.
- 13. **Bourlioux, P., B. Koletzko, F. Guarner, and V. Braesco.** 2003. The intestine and its microflora are partners for the protection of the host: report on the Danone Symposium "The Intelligent Intestine," held in Paris, June 14, 2002. Am J Clin Nutr **78:**675-83.
- 14. Braat, H., P. Stokkers, T. Hommes, D. Cohn, E. Vogels, I. Pronk, A. Spek, A. van Kampen, S. van Deventer, M. Peppelenbosch, and D. Hommes. 2005. Consequence of functional Nod2 and Tlr4 mutations on gene transcription in Crohn's disease patients. J Mol Med 83:601-9.
- 15. **Bruce, K. D., and M. R. Hughes.** 2000. Terminal restriction fragment length polymorphism monitoring of genes amplified directly from bacterial communities in soils and sediments. Mol Biotechnol **16:**261-9.
- 16. Cahill, R. J., C. J. Foltz, J. G. Fox, C. A. Dangler, F. Powrie, and D. B. Schauer. 1997. Inflammatory bowel disease: an immunity-mediated condition triggered by bacterial infection with *Helicobacter hepaticus*. Infect Immun 65:3126-3131.
- 17. **Carlo, E., and D. K. Podolsky.** 2000. Differential alteration in intestinal epithelial cell expression of toll-like receptor 3 (TLR3) and TLR4 in inflammatory bowel disease. Infect Immun **68:**7010-7.
- 18. Chien, C. C., N. S. Taylor, Z. Ge, D. B. Schauer, V. B. Young, and J. G. Fox. 2000. Identification of *cdtB* homologues and cytolethal distending toxin activity in enterohepatic *Helicobacter* spp. J Med Microbiol **49:**525-34.
- 19. Chin, E. Y., C. A. Dangler, J. G. Fox, and D. B. Schauer. 2000.

 Helicobacter hepaticus infection triggers inflammatory bowel disease in T cell receptor alpha/beta mutant mice. Comp Med 50:586-94.
- 20. Clement, B. G., L. E. Kehl, K. L. DeBord, and C. L. Kitts. 1998. Terminal restriction fragment patterns (TRFPs), a rapid, PCR-based

- method for the comparison of complex baccterial communities. Journal of Microbiological Methods **31:**135-142.
- 21. Cole, J. R., B. Chai, T. L. Marsh, R. J. Farris, Q. Wang, S. A. Kulam, S. Chandra, D. M. McGarrell, T. M. Schmidt, G. M. Garrity, and J. M. Tiedje. 2003. The Ribosomal Database Project (RDP-II): previewing a new autoaligner that allows regular updates and the new prokaryotic taxonomy. Nucleic Acids Res 31:442-3.
- Darfeuille-Michaud, A., J. Boudeau, P. Bulois, C. Neut, A. L. Glasser, N. Barnich, M. A. Bringer, A. Swidsinski, L. Beaugerie, and J. F. Colombel. 2004. High prevalence of adherent-invasive Escherichia coli associated with ileal mucosa in Crohn's disease. Gastroenterology 127:412-21.
- 23. Dieleman, L. A., A. Arends, S. L. Tonkonogy, M. S. Goerres, D. W. Craft, W. Grenther, R. K. Sellon, E. Ballsh, and R. B. Sartor. 2000. Helicobacter hepaticus does not induce or potentiate colitis in interleukin-10-deficient mice. Infect Immun 68:5107-13.
- 24. **Dworkin, M., and Springer-Verlag New York Inc.** 1999, posting date. The prokaryotes
- an evolving electronic resource for the microbiological community. Springer-Verlag Release 3. [Online.]
- 25. Eckburg, P. B., E. M. Bik, C. N. Bernstein, E. Purdom, L. Dethlefsen, M. Sargent, S. R. Gill, K. E. Nelson, and D. A. Relman. 2005. Diversity of the human intestinal microbial flora. Science 308:1635-8.
- 26. Elson, C. O., Y. Cong, V. J. McCracken, R. A. Dimmitt, R. G. Lorenz, and C. T. Weaver. 2005. Experimental models of inflammatory bowel disease reveal innate, adaptive, and regulatory mechanisms of host dialogue with the microbiota. Immunol Rev 206:260-76.
- 27. Engle, S. J., I. Ormsby, S. Pawlowski, G. P. Boivin, J. Croft, E. Balish, and T. Doetschman. 2002. Elimination of colon cancer in germ-free transforming growth factor beta 1-deficient mice. Cancer Res 62:6362-6.
- 28. Erdman, S. E., V. P. Rao, T. Poutahidis, M. M. Ihrig, Z. Ge, Y. Feng, M. Tomczak, A. B. Rogers, B. H. Horwitz, and J. G. Fox. 2003. CD4(+)CD25(+) regulatory lymphocytes require interleukin 10 to interrupt colon carcinogenesis in mice. Cancer Res 63:6042-50.

- 29. **Falkow, S.** 2004. Molecular Koch's postulates applied to bacterial pathogenicity—a personal recollection 15 years later. Nat Rev Microbiol **2:**67-72.
- 30. **Farrell, R. J., and J. T. LaMont.** 2002. Microbial factors in inflammatory bowel disease. Gastroenterol Clin North Am **31:41-62**.
- Finlay, B. B., and S. Falkow. 1997. Common themes in microbial pathogenicity revisited. Microbiol Mol Biol Rev 61:136-69.
- 32. Foltz, C. J., J. G. Fox, R. Cahill, J. C. Murphy, L. Yan, B. Shames, and D. B. Schauer. 1998. Spontaneous inflammatory bowel disease in multiple mutant mouse lines: association with colonization by *Helicobacter hepaticus*. Helicobacter 3:69-78.
- 33. **Forney, L. J., X. Zhou, and C. J. Brown.** 2004. Molecular microbial ecology: land of the one-eyed king. Curr Opin Microbiol **7:**210-20.
- 34. **Fox, J. G.** 2002. The non-*H pylori* helicobacters: their expanding role in gastrointestinal and systemic diseases. Gut **50:**273-83.
- 35. Fox, J. G., F. E. Dewhirst, J. G. Tully, B. J. Paster, L. Yan, N. S. Taylor, M. J. Collins, Jr., P. L. Gorelick, and J. M. Ward. 1994. *Helicobacter hepaticus sp. nov.*, a microaerophilic bacterium isolated from livers and intestinal mucosal scrapings from mice. Journal of Clinical Microbiology 32:1238-1245.
- 36. Freter, R. 1955. The fatal enteric cholera infection in the guinea pig, achieved by inhibition of normal enteric flora. J Infect Dis 97:57-65.
- 37. **Freter, R.** 1962. In vivo and in vitro antagonism of intestinal bacteria against Shigellaflexneri. II. The inhibitory mechanism. J Infect Dis **110:**38-46.
- 38. **Freter, R., and A. Ozawa.** 1963. Explanation For Limitation Of Populations Of Escherichia Coli In Broth Cultures. J Bacteriol **86:**904-10.
- 39. **Fuss, I. J., M. Boirivant, B. Lacy, and W. Strober.** 2002. The interrelated roles of TGF-beta and IL-10 in the regulation of experimental colitis. J Immunol **168:900-8**.
- 40. **Ge, Z., Y. Feng, M. T. Whary, P. R. Nambiar, S. Xu, V. Ng, N. S. Taylor, and J. G. Fox.** 2005. Cytolethal distending toxin is essential for *Helicobacter hepaticus* colonization in outbred Swiss Webster mice. Infect Immun **73:**3559-67.

- 41. **Ge, Z., D. A. White, M. T. Whary, and J. G. Fox.** 2001. Fluorogenic PCR-based quantitative detection of a murine pathogen, *Helicobacter hepaticus*. J Clin Microbiol **39:**2598-602.
- 42. Gionchetti, P., F. Rizzello, A. Venturi, P. Brigidi, D. Matteuzzi, G. Bazzocchi, G. Poggioli, M. Miglioli, and M. Campieri. 2000. Oral bacteriotherapy as maintenance treatment in patients with chronic pouchitis: a double-blind, placebo-controlled trial. Gastroenterology 119:305-9.
- 43. **Good, I. J.** 1953. The population frequencies of species and the estimation of population parameters. Biometrica **40:**237-264.
- 44. **Hayashi, H., M. Sakamoto, and Y. Benno.** 2002. Phylogenetic analysis of the human gut microbiota using 16S rDNA clone libraries and strictly anaerobic culture-based methods. Microbiol Immunol **46**:535-48.
- 45. **Heck, K. J. J., and G. V. Belle.** 1975. Explicit calculation of the rarefaction diversity measurement and the determination of sufficient sample size. Ecology **56**:1459-1461.
- 46. **Heczko, U., A. Abe, and B. B. Finlay.** 2000. Segmented filamentous bacteria prevent colonization of enteropathogenic *Escherichia coli* O103 in rabbits. J Infect Dis **181:**1027-33.
- 47. Hoentjen, F., H. J. Harmsen, H. Braat, C. D. Torrice, B. A. Mann, R. B. Sartor, and L. A. Dieleman. 2003. Antibiotics with a selective aerobic or anaerobic spectrum have different therapeutic activities in various regions of the colon in interleukin 10 gene deficient mice. Gut 52:1721-7.
- 48. Hoentjen, F., G. W. Welling, H. J. Harmsen, X. Zhang, J. Snart, G. W. Tannock, K. Lien, T. A. Churchill, M. Lupicki, and L. A. Dieleman. 2005. Reduction of colitis by prebiotics in HLA-B27 transgenic rats is associated with microflora changes and immunomodulation. Inflamm Bowel Dis 11:977-85.
- 49. Hold, G. L., S. E. Pryde, V. J. Russell, E. Furrie, and H. J. Flint. 2002. Assessment of microbial diversity in human colonic samples by 16S rDNA sequence analysis. FEMS Microbiology Ecology 39:33-39.
- 50. Holdeman, L. V., I. J. Good, and W. E. Moore. 1976. Human fecal flora: variation in bacterial composition within individuals and a possible effect of emotional stress. Appl Environ Microbiol 31:359-75.

- 51. Holst, E., A. R. Goffeng, and B. Andersch. 1994. Bacterial vaginosis and vaginal microorganisms in idiopathic premature labor and association with pregnancy outcome. J Clin Microbiol 32:176-86.
- 52. **Hooper, L. V.** 2004. Bacterial contributions to mammalian gut development. Trends Microbiol **12:129-34**.
- Hopkins, M. J., R. Sharp, and G. T. Macfarlane. 2001. Age and disease related changes in intestinal bacterial populations assessed by cell culture, 16S rRNA abundance, and community cellular fatty acid profiles. Gut 48:198-205.
- 54. **Humlova, Z.** 2004. [Bacteria and their role in allergic diseases]. Cas Lek Cesk **143:**21-5.
- 55. **Jussi, V., E. Erkki, and T. Paavo.** 2005. Comparison of cellular fatty acid profiles of the microbiota in different gut regions of BALB/c and C57BL/6J mice. Antonie Van Leeuwenhoek **88:**67-74.
- 56. **Kibe, R., M. Sakamoto, H. Hayashi, H. Yokota, and Y. Benno.** 2004. Maturation of the murine cecal microbiota as revealed by terminal restriction fragment length polymorphism and 16S rRNA gene clone libraries. FEMS Microbiol Lett **235**:139-46.
- 57. Kleessen, B., A. J. Kroesen, H. J. Buhr, and M. Blaut. 2002. Mucosal and invading bacteria in patients with inflammatory bowel disease compared with controls. Scand J Gastroenterol 37:1034-41.
- 58. Kuehl, C. J., H. D. Wood, T. L. Marsh, T. M. Schmidt, and V. B. Young. 2005. Colonization of the cecal mucosa by Helicobacter hepaticus impacts the diversity of the indigenous microbiota. Infect Immun 73:6952-61.
- 59. Kullberg, M. C., J. M. Ward, P. L. Gorelick, P. Caspar, S. Hieny, A. Cheever, D. Jankovic, and A. Sher. 1998. Helicobacter hepaticus triggers colitis in specific-pathogen-free interleukin-10 (IL-10)-deficient mice through an IL-12- and gamma interferon-dependent mechanism. Infect Immun 66:5157-66.
- 60. Kumar, S., K. Tamura, and M. Nei. 2004. MEGA3: Integrated software for Molecular Evolutionary Genetics Analysis and sequence alignment. Brief Bioinform 5:150-63.

- 61. Lara-Tejero, M., and J. E. Galan. 2002. Cytolethal distending toxin: limited damage as a strategy to modulate cellular functions. Trends in Microbiology 10:147-52.
- 62. Leser, T. D., J. Z. Amenuvor, T. K. Jensen, R. H. Lindecrona, M. Boye, and K. Moller. 2002. Culture-independent analysis of gut bacteria: the pig gastrointestinal tract microbiota revisited. Appl Environ Microbiol 68:673-90.
- 63. Ley, R. E., F. Backhed, P. Turnbaugh, C. A. Lozupone, R. D. Knight, and J. I. Gordon. 2005. Obesity alters gut microbial ecology. Proc Natl Acad Sci U S A 102:11070-5.
- 64. Llu, W. T., T. L. Marsh, H. Cheng, and L. J. Forney. 1997.

 Characterization of microbial diversity by determining terminal restriction fragment length polymorphisms of genes encoding 16S rRNA. Appl Environ Microbiol 63:4516-22.
- 65. **Macdonald, T. T., and G. Monteleone.** 2005. Immunity, inflammation, and allergy in the gut. Science **307:**1920-5.
- 66. Madsen, K. L., J. S. Doyle, L. D. Jewell, M. M. Tavernini, and R. N. Fedorak. 1999. Lactobacillus species prevents colitis in interleukin 10 gene-deficient mice. Gastroenterology 116:1107-14.
- 67. Madsen, K. L., J. S. Doyle, M. M. Tavernini, L. D. Jewell, R. P. Rennie, and R. N. Fedorak. 2000. Antibiotic therapy attenuates colitis in interleukin 10 gene-deficient mice. Gastroenterology 118:1094-105.
- Maggio-Price, L., H. Bielefeldt-Ohmann, P. Treuting, B. M. Iritani, W. Zeng, A. Nicks, M. Tsang, D. Shows, P. Morrissey, and J. L. Viney. 2005. Dual infection with Helicobacter bilis and Helicobacter hepaticus in p-glycoprotein-deficient mdr1a-/- mice results in colitis that progresses to dysplasia. Am J Pathol 166:1793-806.
- 69. **Mahida, Y. R., and V. E. Rolfe.** 2004. Host-bacterial interactions in inflammatory bowel disease. Clin Sci (Lond) **107:**331-41.
- 70. Manichanh, C., L. Rigottier-Gois, E. Bonnaud, K. Gloux, E. Pelletier, L. Frangeul, R. Nalin, C. Jarrin, P. Chardon, P. Marteau, J. Roca, and J. Dore. 2005. Reduced diversity of faecal microbiota in Crohn's disease revealed by a metagenomic approach. Gut.
- 71. **Marsh, T. L.** 1999. Terminal restriction fragment length polymorphism (T-RFLP): an emerging method for characterizing diversity among

- homologous populations of amplification products. Current Opinion in Microbiology 2:323-7.
- 72. Martin, H. M., B. J. Campbell, C. A. Hart, C. Mpofu, M. Nayar, R. Singh, H. Englyst, H. F. Williams, and J. M. Rhodes. 2004. Enhanced Escherichia coli adherence and invasion in Crohn's disease and colon cancer. Gastroenterology 127:80-93.
- 73. **Mathew, C. G., and C. M. Lewis.** 2004. Genetics of inflammatory bowel disease: progress and prospects. Hum Mol Genet **13 Spec No 1:**R161-8.
- 74. Matsumoto, S., T. Hara, T. Hori, K. Mitsuyama, M. Nagaoka, N. Tomiyasu, A. Suzuki, and M. Sata. 2005. Probiotic Lactobacillus-induced improvement in murine chronic inflammatory bowel disease is associated with the down-regulation of pro-inflammatory cytokines in lamina propria mononuclear cells. Clin Exp Immunol 140:417-26.
- 75. McBurney, W., M. Mangold, K. Munro, M. Schultz, H. C. Rath, and G. W. Tannock. 2006. PCR/DGGE and 16S rRNA gene library analysis of the colonic microbiota of HLA-B27/beta2-microglobulin transgenic rats. Lett Appl Microbiol 42:165-71.
- 76. **McCracken, V. J., and R. G. Lorenz.** 2001. The gastrointestinal ecosystem: a precarious alliance among epithelium, immunity and microbiota. Cell Microbiol 3:1-11.
- 77. **Moore, W. E., and L. V. Holdeman.** 1974. Human fecal flora: the normal flora of 20 Japanese-Hawaiians. Appl Microbiol **27:**961-79.
- 78. Mueller, S., K. Saunier, C. Hanisch, E. Norin, L. Alm, T. Midtvedt, A. Cresci, S. Silvi, C. Orpianesi, M. C. Verdenelli, T. Clavel, C. Koebnick, H. J. Zunft, J. Dore, and M. Blaut. 2006. Differences in fecal microbiota in different European study populations in relation to age, gender, and country: a cross-sectional study. Appl Environ Microbiol 72:1027-33.
- 79. **Mylonaki, M., N. B. Rayment, D. S. Rampton, B. N. Hudspith, and J. Brostoff.** 2005. Molecular characterization of rectal mucosa-associated bacterial flora in inflammatory bowel disease. Inflamm Bowel Dis 11:481-7.
- 80. **Mylonakis, E., E. T. Ryan, and S. B. Calderwood.** 2001. Clostridium difficile--Associated diarrhea: A review. Arch Intern Med **161**:525-33.

- 81. **Noverr, M. C., and G. B. Huffnagle.** 2005. The 'microflora hypothesis' of allergic diseases. Clin Exp Allergy **35:**1511-20.
- 82. **Noverr, M. C., R. M. Noggle, G. B. Toews, and G. B. Huffnagle.** 2004. Role of antibiotics and fungal microbiota in driving pulmonary allergic responses. Infect Immun **72:**4996-5003.
- 83. **Ohara, M., E. Oswald, and M. Sugai.** 2004. Cytolethal distending toxin: a bacterial bullet targeted to nucleus. J Biochem (Tokyo) **136**:409-13.
- 84. Oswald, E., J. P. Nougayrede, F. Taieb, and M. Sugai. 2005. Bacterial toxins that modulate host cell-cycle progression. Curr Opin Microbiol 8:83-91.
- 85. Ott, S. J., M. Musfeldt, D. F. Wenderoth, J. Hampe, O. Brant, U. R. Folsch, K. N. Timmis, and S. Schreiber. 2004. Reduction in diversity of the colonic mucosa associated bacterial microflora in patients with active inflammatory bowel disease. Gut 53:685-93.
- 86. **Pace, N. R.** 1997. A molecular view of microbial diversity and the biosphere. Science **276:734-40**.
- 87. **Peek, R. M., Jr., and M. J. Blaser.** 2002. *Helicobacter pylori* and gastrointestinal tract adenocarcinomas. Nat Rev Cancer 2:28-37.
- 88. Pena, J. A., A. B. Rogers, Z. Ge, V. Ng, S. Y. Li, J. G. Fox, and J. Versalovic. 2005. Probiotic Lactobacillus spp. diminish Helicobacter hepaticus-induced inflammatory bowel disease in interleukin-10-deficient mice. Infect Immun 73:912-20.
- 89. **Pratt, J. S., K. L. Sachen, H. D. Wood, K. A. Eaton, and V. B. Young.** 2006. Modulation of host immune responses by the cytolethal distending toxin of Helicobacter hepaticus. Infect Immun **74**:4496-504.
- 90. **Prindiville, T., M. Cantrell, and K. H. Wilson.** 2004. Ribosomal DNA sequence analysis of mucosa-associated bacteria in Crohn's disease. Inflamm Bowel Dis 10:824-33.
- 91. **Pryde, S. E., S. H. Duncan, G. L. Hold, C. S. Stewart, and H. J. Flint.** 2002. The microbiology of butyrate formation in the human colon. FEMS Microbiol Lett **217:133-9**.

- 92. Rakoff-Nahoum, S., J. Paglino, F. Eslami-Varzaneh, S. Edberg, and R. Medzhitov. 2004. Recognition of commensal microflora by toll-like receptors is required for intestinal homeostasis. Cell 118:229-41.
- 93. **Ricke, P., S. Kolb, and G. Braker.** 2005. Application of a newly developed ARB software-integrated tool for in silico terminal restriction fragment length polymorphism analysis reveals the dominance of a novel pmoA cluster in a forest soil. Appl Environ Microbiol **71:**1671-3.
- 94. Sakamoto, M., Y. Huang, M. Ohnishi, M. Umeda, I. Ishikawa, and Y. Benno. 2004. Changes in oral microbial profiles after periodontal treatment as determined by molecular analysis of 16S rRNA genes. J Med Microbiol 53:563-71.
- 95. **Sakamoto, M., M. Umeda, and Y. Benno. 2005.** Molecular analysis of human oral microbiota. J Periodontal Res **40:**277-85.
- 96. Salzman, N. H., H. De Jong, Y. Paterson, H. J. Harmsen, G. W. Welling, and N. A. Bos. 2002. Analysis of 16S libraries of mouse gastrointestinal microflora reveals a large new group of mouse intestinal bacteria. Microbiology 148:3651-3660.
- 97. **Sartor, R. B.** 2005. Probiotic therapy of intestinal inflammation and infections. Curr Opin Gastroenterol **21:44-50**.
- 98. **Sartor, R. B.** 2003. Targeting enteric bacteria in treatment of inflammatory bowel diseases: why, how, and when. Curr Opin Gastroenterol **19:**358-65.
- 99. **Schloss, P. D., and J. Handelsman.** 2005. Introducing DOTUR, a computer program for defining operational taxonomic units and estimating species richness. Appl Environ Microbiol **71:**1501-6.
- 100. Schloss, P. D., B. R. Larget, and J. Handelsman. 2004. Integration of microbial ecology and statistics: a test to compare gene libraries. Appl Environ Microbiol 70:5485-92.
- 101. **Schmidt, T. M., and D. A. Relman.** 1994. Phylogenetic identification of uncultured pathogens using ribosomal RNA sequences. Methods Enzymol **235**:205-22.
- 102. **Seguritan, V., and F. Rohwer.** 2001. FastGroup: a program to dereplicate libraries of 16S rDNA sequences. BMC Bioinformatics **2:**9.

- 103. Singleton, D. R., M. A. Furlong, S. L. Rathbun, and W. B. Whitman. 2001. Quantitative comparisons of 16S rRNA gene sequence libraries from environmental samples. Appl Environ Microbiol 67:4374-6.
- 104. **Solnick, J. V., and D. B. Schauer.** 2001. Emergence of diverse *Helicobacter* species in the pathogenesis of gastric and enterohepatic diseases. Clin Microbiol Rev 14:59-97.
- 105. **Stallmach, A., and O. Carstens.** 2002. Role of infections in the manifestation or reactivation of inflammatory bowel diseases. Inflamm Bowel Dis **8:**213-8.
- 106. Strober, W., B. Kelsall, I. Fuss, T. Marth, B. Ludviksson, R. Ehrhardt, and M. Neurath. 1997. Reciprocal IFN-gamma and TGF-beta responses regulate the occurrence of mucosal inflammation. Immunol Today 18:61-4.
- 107. Suau, A., R. Bonnet, M. Sutren, J. J. Godon, G. R. Gibson, M. D. Collins, and J. Dore. 1999. Direct analysis of genes encoding 16S rRNA from complex communities reveals many novel molecular species within the human gut. Appl Environ Microbiol 65:4799-807.
- 108. Suerbaum, S., C. Josenhans, T. Sterzenbach, B. Drescher, P. Brandt, M. Bell, M. Droge, B. Fartmann, H. P. Fischer, Z. Ge, A. Horster, R. Holland, K. Klein, J. Konig, L. Macko, G. L. Mendz, G. Nyakatura, D. B. Schauer, Z. Shen, J. Weber, M. Frosch, and J. G. Fox. 2003. The complete genome sequence of the carcinogenic bacterium *Helicobacter hepaticus*. Proc Natl Acad Sci U S A 100:7901-6.
- 109. Swidsinski, A., V. Loening-Baucke, H. Lochs, and L. P. Hale. 2005. Spatial organization of bacterial flora in normal and inflamed intestine: a fluorescence in situ hybridization study in mice. World J Gastroenterol 11:1131-40.
- 110. Taurog, J. D., J. A. Richardson, J. T. Croft, W. A. Simmons, M. Zhou, J. L. Fernandez-Sueiro, E. Balish, and R. E. Hammer. 1994. The germfree state prevents development of gut and joint inflammatory disease in HLA-B27 transgenic rats. J Exp Med 180:2359-64.
- 111. **Tilman, D.** 2004. Niche tradeoffs, neutrality, and community structure: a stochastic theory of resource competition, invasion, and community assembly. Proc Natl Acad Sci U S A **101:**10854-61.
- 112. Tlaskalova-Hogenova, H., R. Stepankova, T. Hudcovic, L. Tuckova, B. Cukrowska, R. Lodinova-Zadnikova, H. Kozakova, P. Rossmann, J.

- Bartova, D. Sokol, D. P. Funda, D. Borovska, Z. Rehakova, J. Sinkora, J. Hofman, P. Drastich, and A. Kokesova. 2004. Commensal bacteria (normal microflora), mucosal immunity and chronic inflammatory and autoimmune diseases. Immunol Lett 93:97-108.
- 113. **Toivanen, P., J. Vaahtovuo, and E. Eerola.** 2001. Influence of major histocompatibility complex on bacterial composition of fecal flora. Infect Immun **69:**2372-7.
- 114. Verhelst, R., H. Verstraelen, G. Claeys, G. Verschraegen, J. Delanghe, L. Van Simaey, C. De Ganck, M. Temmerman, and M. Vaneechoutte. 2004. Cloning of 16S rRNA genes amplified from normal and disturbed vaginal microflora suggests a strong association between Atopobium vaginae, Gardnerella vaginalis and bacterial vaginosis. BMC Microbiol 4:16.
- 115. **Vollaard, E. J., and H. A. Clasener.** 1994. Colonization resistance. Antimicrob Agents Chemother **38:**409-14.
- 116. **von Wintzingerode, F., U. B. Gobel, and E. Stackebrandt.** 1997. Determination of microbial diversity in environmental samples: pitfalls of PCR-based rRNA analysis. FEMS Microbiol Rev **21:**213-29.
- 117. Ward, J. M., M. R. Anver, D. C. Haines, and R. E. Benveniste. 1994. Chronic active hepatitis in mice caused by *Helicobacter hepaticus*. American Journal of Pathology **145**:959-968.
- 118. Whary, M. T., J. H. Cline, A. E. King, C. A. Corcoran, S. Xu, and J. G. Fox. 2000. Containment of *Helicobacter hepaticus* by use of husbandry practices. Comp Med **50:**78-81.
- 119. **Wilson, K. H., and R. B. Blitchington.** 1996. Human colonic biota studied by ribosomal DNA sequence analysis. Appl Environ Microbiol **62:**2273-8.
- 120. Young, V. B., C. C. Chien, K. A. Knox, N. S. Taylor, D. B. Schauer, and J. G. Fox. 2000. Cytolethal distending toxin in avian and human isolates of *Helicobacter pullorum*. J Infect Dis 182:620-3.
- 121. Young, V. B., K. A. Knox, J. S. Pratt, J. S. Cortez, L. S. Mansfield, A. B. Rogers, J. G. Fox, and D. B. Schauer. 2004. In vitro and in vivo characterization of Helicobacter hepaticus cytolethal distending toxin mutants. Infect Immun 72:2521-7.

- 122. Young, V. B., K. A. Knox, and D. B. Schauer. 2000. Cytolethal distending toxin sequence and activity in the enterohepatic pathogen *Helicobacter hepaticus*. Infection & Immunity **68**:184-191.
- 123. **Young, V. B., and T. M. Schmidt.** 2004. Antibiotic-associated diarrhea accompanied by large-scale alterations in the composition of the fecal microbiota. J Clin Microbiol **42:1**203-6.
- 124. **Zoetendal, E. G., A. D. Akkermans, and W. M. De Vos.** 1998. Temperature gradient gel electrophoresis analysis of 16S rRNA from human fecal samples reveals stable and host-specific communities of active bacteria. Appl Environ Microbiol **64:**3854-9.
- 125. **Zoetendal, E. G., C. T. Collier, S. Koike, R. I. Mackie, and H. R. Gaskins.** 2004. Molecular ecological analysis of the gastrointestinal microbiota: a review. J Nutr **134**:465-72.

